AERIAL PLATFORMS UTILIZATION FOR FUTURE NETWORKS

A THESIS SUBMITTED TO
THE GRADUATE SCHOOL OF
ENGINEERING AND NATURAL SCIENCES
OF ISTANBUL MEDIPOL UNIVERSITY
IN PARTIAL FULFILLMENT OF THE REQUIREMENTS FOR
THE DEGREE OF
MASTER OF SCIENCE
IN
ELECTRICAL, ELECTRONICS ENGINEERING AND CYBER SYSTEMS

By
Mostafa Helmy Mohamed
March, 2018

ABSTRACT

AERIAL PLATFORMS UTILIZATION FOR FUTURE NETWORKS

Mostafa Helmy Mohamed
M.S. in Electrical, Electronics Engineering and Cyber Systems
Advisor: Prof. Dr. Hüseyin Arslan
March, 2018

Challenges facing the next generation of communication systems include utilizing the wireless networks in the rural areas and disaster situations, as well as the requirements of high capacity services and connectivity wherever, whenever, and however necessary. With the limitations on the current terrestrial and satellite backbones, utilizing the aerial platforms as a spine of wireless communication is a promising solution. For disastrous scenarios, we address the issue of optimizing the location of aerial base stations (ABS) to provide minimum power consumption due to path-loss. We propose an algorithm that dynamically positions ABS in low altitude platform (LAP) by moving the ABS between multiple points within the whole coverage area. Furthermore, we derive the outage probability formula for each user to measure how much gain this algorithm can offer. For improving the performance of wireless communication in future networks, we study the behavior of the aerial heterogeneous networks that utilize high and low altitude platforms (HAPs, LAPs) working on the same network as macro- and femto- cells, respectively. For that model, we derive the coverage probability for the signal to interference ratio (SIR) in the cases where, either the downlink channels are correlated or uncorrelated with respect to shadowing. The results show the coverage was enhanced due to the effect of correlated shadowing between HAPs and LAPs coverage area. Also, for each user, we use the previous scenario to determine the probability of being associated with either one of the HAP or LAP. From the association probability, we derive the cell load of each ABS. After that, we develop a framework of the outage probability for a target user for a certain platform. Finally, we propose a dynamic placement algorithm for LAPs ABSs, to achieve load balancing and improve the quality of service (QoS) for overall users. We show, through simulation results, that the algorithm provides considerable gains over static aerial cellular networks.

Keywords: Aerial Heterogeneous Cellular Networks, Disaster Scenarios, Unmanned Aerial Vehicles, ABS, HAP, LAP, Correlated Shadowing.

ÖZET

GELECEK AĞLAR IÇIN HAVA PLATFORMLARI KULLANIMI

Mostafa Helmy Mohamed
Elektrik-Elektronik Mühendisliği ve Siber Sistemler, Yüksek Lisans
Tez Danışmanı: Prof. Dr. Hüseyin Arslan
Mart, 2018

Yeni nesil iletişim sistemlerinin karşılaştıkları zorluklar arasında, kırsal alanlarda ve felaket durumlarında kablosuz ağların kullanılması ile nerede, ne zaman ve nasıl olursa olsun yüksek kapasiteli hizmetlerin ve bağlantıların gereklilikleri yer almaktadır. Mevcut yerleşik karasal ve uydu haberleşmelerindeki sınırlamalardan dolayı kablosuz iletişimin bir temel taşı olarak hava platformlarını kullanmak umut verici bir çözümdür. ABS'yi alçak irtifa platformunda (LAP) dinamik olarak konumlandıran ve tüm kapsama alanı içinde birçok nokta arasında hareket ettiren bir algoritma önerdik. Ayrıca, bu algoritmanın ne kadar kazanç sağlayabileceğini ölçmek için her kullanıcı için kesinti olasılık formülünü türettik. Gelecekteki ağlarda kablosuz iletişim performansını artırmak için, aynı ağ üzerinde çalışan yüksek ve alçak irtifa platformlarını (HAP'ler, LAP'ler) kullanan hava heterojen ağlarının davranışlarını makro ve femto hücrelerde inceledik. Bu model için, uydu-yer hattı(downlink) kanallarının gölgelemeyle ilişkili ya da ilişkisiz olduğu durumlarda sinyal-girişim oranını (SIR) kapsama olasılığını elde ettik. Sonuçlar, HAP ve LAP'ların kapsama alanları arasındaki korelasyonlu gölgelemenin etkisiyle geliştirilmiş göstermektedir. Ayrıca, her kullanıcı için, stokastik geometri kullanarak ilişkili olma olasılığını belirlemek için önceki senaryoyu kullandık. Ilişkilendirme olasılığından, her bir ABS'nin hücre yükünü kullandık. Sonrasında ise belirli bir platform ve hedef kullanıcı için kesinti olasılığının çerçevesini belirledik. Son olarak, HAP kapsama alanındaki yük dengelemeyi sağlamak ve genel kullanıcılar için hizmet kalitesini (QoS) iyileştirmek için LAP'lerin oluşturduğu hücrelerde dinamik bir yerleştirme ve boyutlandırma algoritması önerdik. Simülasyon sonuçları aracılığıyla, algoritmanın statik hava hücresel ağları üzerinde önemli kazançlar sağladığını gösterdik.

Anahtar sözcükler: Hava Heterojen Hücresel Ağlar, Ykıcı Senaryolar, Insansız Hava Araçları, ABS, HAP, LAP, Ilişkili Gölgeleme.

Acknowledgement

First, I would like to thank my advisor Dr. Hüseyin Arslan for his guidance, encouragement and support throughout my study. I wish to thank Dr. Tunçer Baykaş for offering valuable suggestions.

It has been a privilege to join the Communication, Signal processing and Networking Center (CoSiNC). I would like to thank my friends Marwan Yusuf, Morteza Soltani, Zekeriya Esat, Murat Karabacak, Mostafa Ibrahim and Jehad Hamamreh from our research group for their support as friends and for sharing their knowledge as colleagues. Special thank for Marwan Yusuf for all of his support.

Last but by no means least, I would like to thank my parents for their continued support, encouragement and sacrifice throughout the years, and I will be forever indebted to them for all that they have done.

Contents

List of Figures

List of Tables

Chapter 1

Introduction

The growth in demand of wireless communications market over the last two decades offers a strong movement from voice-oriented wireless servers to huge data rates and a wide variety of applications. However, for achieving that objective, we should pay attention to the limited resources available such as bandwidth. Furthermore, in the cellular networks, the communication could be destroyed in the case of disasters such as earthquakes or floods. Currently, available disaster recovery backhaul telecommunications systems are inadequate for saving people lives, since the collapse of telecommunications systems during disaster situations leads to the loss of many lives. To meet all of those challenges, it is necessary to find instant solutions using the suitable resources.

Aerial platforms have attracted the attention of both telecommunication scientists and the industry to provide communications-based aerial base stations. Due to the big progress in the aerial platforms technology, (i.e. increased carrying capacity that can operate at different altitudes with several tasks, more lifetime fight, better control management techniques, and the ability to use solar energy), aerial platforms can perform a variety of missions such as surveillance, positioning, and cellular networks [1]. Also, due to fast deployment, they can scatter in the disaster areas within minimum time [2].

In the last two decades, long endurance high altitude platforms (HAP) that are operating at altitudes of $17-22$ km, have attracted most of the industrial and academic researchers

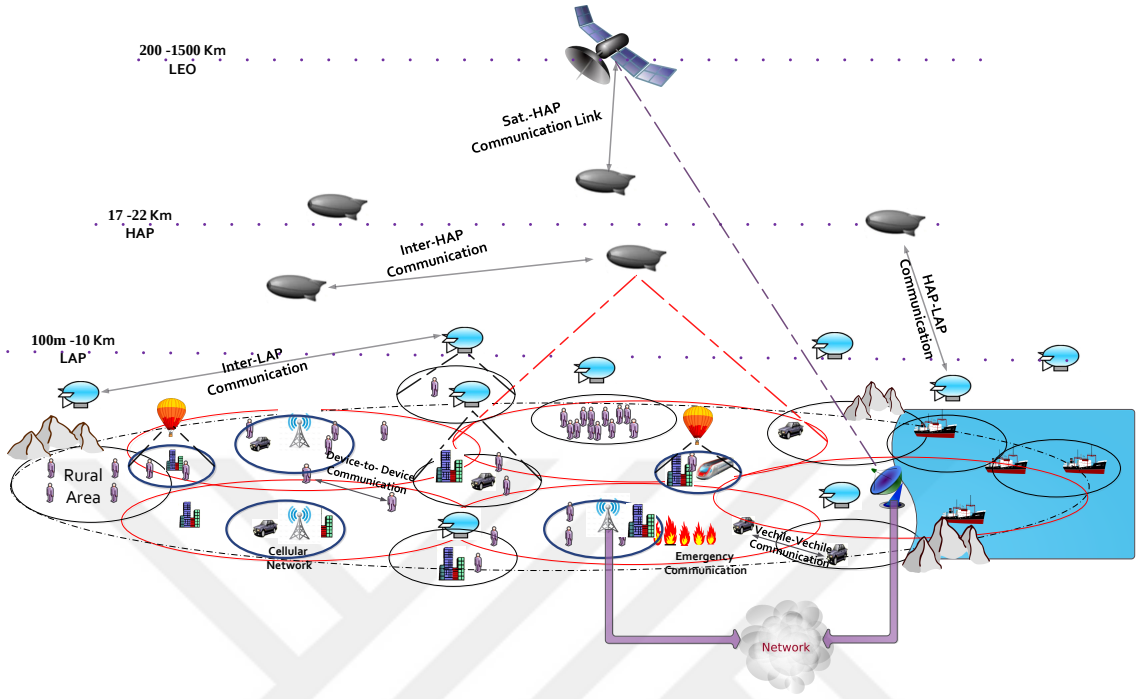

Figure 1.1: Complete aerial-terrestrial heterogeneous wireless cellular architecture

[3]. Recently, other types have been developed to operate at lower altitudes of 100 m -10 km [4, 5]. These platforms, collected under the category of low altitude platforms (LAP) like ABSOLUTE project, have the potential to effectively complement terrestrial or satellite telecommunication networks [6]. Since they are working at low altitudes, they are easy to deploy and close to the concept of broadband cellular networks, so they can combine both optimum coverage and restricted cell radius [7]. For those platforms (HAPs & LAPs), applied standards could be Wi-Fi, Wi-MAX, LTE-A or GSM [4].

Furthermore, studying the combination of those platforms with terrestrial-satellite network architecture as illustrated in Fig. 1.1 is not comprehensively investigated in the current state-of-the-art. This is very critical, because establishing an ABS-based cellular network introduces new challenges compared to the classical cellular networks. First, the channel model will be based on probabilistic LOS and NLOS links [8, 9]. Second, unlike conventional fixed BSs, the height of an ABS is adjustable and impact the coverage performance [10]. To that end, practical approaches that make use of all those platforms as a

promising solution have been investigated.

During disaster situations, emergency networks face tough constraints regarding their total energy consumption. Indeed, the emergency communication network should guarantee an energy efficient process to maximize the disaster areas survivability. Moreover, the energy consumption for the links between ground and LAPs, which depends on the quality and the availability of the channel, must be carefully investigated and optimized. The authors in [8] propose a cooperative strategy algorithm for uplink and downlink communications channels by considering the positions of the relay nodes in the environment and selecting the best relay link which minimizes the overall energy consumption. In [11], the authors consider a cluster of nodes cooperating together and analyze the corresponding energy efficiency due to cooperation. However, they consider those relays have fixed positions in the air and optimize the energy consumption depending on the number of relays. A new algorithm is proposed for adapting the position of ABS to support minimum power consumption by minimizing the total pathloss of subscribers. In Chapter 3 [1], we present a real-time and dynamic algorithm which decreases the energy consumption for aerial-terrestrial networks by adapting the location of ABS based on the channel conditions. Also, we derive the outage probability formula with respect to the shadowing fade margin for each user to measure how much gain this algorithm can offer.

Although the usage of high and low altitude platforms (HAPs, LAPs) provide a promising solution for future wireless communication systems, incorporating these platforms in a heterogeneous network has not been well studied so far in the literature. In particular, an analytical evaluation of this coexistence, such as total coverage, is lacking in the current state-of-the-art. In Chapter 4 [2], we develop an analytical framework for evaluating the coverage probability in aerial heterogeneous cellular networks (AHCNs) with considering the shadow fading effect. We also show the impact of correlated interferers platforms on the coverage probability.

Future telecommunication systems should be able to serve a wide variety of users, anytime and anywhere. One of the key concepts to efficiently use the available resources to

[1] This work is published in [12].
[2] This work is published in [13].

meet such demands is heterogeneous cellular networks (HCNs) [14]. By coordinating various type of cells, e.g. macro-, micro- and femto-cells, in the same area, HCNs offer a very flexible structure compared to conventional macro-only systems. Carrying out such a coordination requires considering the transmit powers, coverage areas and spectral resources of different base stations (BSs) and assigning users to the proper BSs based on their requirements. The literature usually referred to this as the user association problem and plays a critical role in improving the load balancing, energy and spectrum efficiency in HCNs [15, 16]. In Chapter 5 [3], for AHCN, we derive the corresponding association probability. This probability helps us to calculate the cell load in each platform. Then we drive a framework of the outage probability for a target user for a certain platform. After that we introduce an algorithm for positioning the LAPs in order to achieve load balancing and increase the total throughput of such network.

1.1 Organization of Thesis

This thesis consists of six chapters. An overview of aerial platforms is provided in Chapter 2. Chapter 3 introduces the utilization of LAPs to enhance the wireless communication links and energy efficiency in disaster areas. A dynamic algorithm which attempts to maximize the received power at ABS by moving it between multiple points within its coverage area is provided. Furthermore, outage probability formula for each user has been derived to measure how much gain this algorithm can offer in LOS and NLOS cases and simulation results are given at the end of the chapter. In Chapter 4, a brief overview of aerial heterogeneous cellular networks is provided, followed by coverage analysis for a typical user in the cases where, the downlinks paths (HAP & LAP) are either correlated or uncorrelated and the effect of elevation angles between high altitude and low altitude platforms on the performance. In Chapter 5, the probability of a typical user to be associated with a LAP or a HAP, is calculated. Then, the average number of users associated with an ABS is derived for HAPs and LAPs. After that, we derive the outage probability for a target user for a certain platform. We also propose a dynamic utilization algorithm for LAPs in an AHCN. Finally, Chapter 6 provides the discussion and a brief summary of the thesis.

[3] This work is published in [17] and extended in [13].

Chapter 2

An Overview Of Aerial Platforms

In this chapter, we provide a summary of the background of aerial platforms. We are going to present some definitions, specifications, types and applications of the aerial platforms. Then, we provide a comparison between terrestrial and aerial platforms systems showing the merits and demerits of each system. Finally, an overview of selected projects and industry research related to aerial platforms will be introduced.

2.1 Definitions and Specifications

Aerial platforms consist of **aerostats** or **aerodynes**, such as tethered, Helikite, a hybrid kite, balloons, airships, quad-copters, manned and unmanned aerial vehicles (UAVs), which are deployed at different altitudes with various missions. An aerostat family is lighter than air aircraft and gets its lift by using a buoyant gas. They can be loaded with a gas of relatively lower-density than the surrounding air such as helium, hydrogen, or hot air. Aerostats contain powered airships and unpowered balloons or tethered. Furthermore, they can carry small scale payloads up to 10 kg that can be handled by the ground stations. An aerodyne family is heavier than aircraft, such as airplanes, UAVs, and quad-copters. They get their lift by finding some ways of pushing air or gas down, so a response happens to lift the aircraft up. There are two methods to generate the dynamic upthrust: powered

lift that come from the engine thrust, or the aerodynamic lift that come from fixed-wing aircraft.

High Altitude Platforms (HAPs) operate at the altitudes 17 - 22 km. They can be airships, planes or UAVs. They can be quite promising for many types of future applications due to their various benefits in operating situations, such as the ability to have a hybrid power of solar and fuel, stability (because of the low wind speeds at those altitudes), payloads up to 1 ton and long endurance. At this altitude, they can provide the best wireless communications features of both satellite and terrestrial, and remote sensing services. However, they have very limited number due to funding-related and technological constraints [18].

Low Altitude Platforms (LAPs) operate at the altitudes 100 m - 10 km. LAPs are easier and faster to deploy than HAPs. They are also closer to the concept of the broadband cellular networks since low altitude combines the optimum coverage and bounded cell radius. Also, they can perform multiple operations at varying altitudes, and they have acceptable communication payloads (up to 10 kg) [6].

2.2 Aerial Platforms Types

2.2.1 HAPs

There are many types of platforms that can be used at high altitudes which were introduced in the last two decades as a solution for wireless communications services in terms of coverage and capacity. All of the HAPs types are under the aerostats or aerodynes families with different characteristics. For example, Figure 2.1 [1] shows the high-altitude aerostats unmanned balloons type which can reach a height between 18 to 37 km.
QinetiQs Zephyr in Figure 2.2 [2] is a solar powered UAV that can stay up for days. It is carried by batteries that can be charged by solar power during the day. Then during the

[1] Image source: http://archives.starbulletin.com/2007/02/01/news/story05.html.
[2] Image source: http://www.qinetiq.com/news/pressreleases/Pages/zephyr-sets-world-record.aspx.

Figure 2.1: High altitude balloons

night, this stored power is used for keeping it in the air. However, the payload abilities are restricted to a maximum of a 1 kg payload.

Figure 2.2: QinetiQs zephyr aircraft

Another example is the High Altitude Long Endurance-Demonstrator (HALE-D) airship, shown in Figure 2.3 [3]. It is designed to be able to reach up to 100 km altitude as the demonstrator is filled with helium and also it has a solar-powered design.

[3]Image source: www.lockheedmartin.com/us/ms2/features/110728-high-altitude-airship-demonstrates-successful-launch-during-abbr.html.

Figure 2.3: High altitude long endurance-demonstrator

Figure 2.4 [4] shows the Global Hawk air vehicle which is designed for high-altitude, Long Endurance UAVs to support data from or to anywhere within the service area during day or night. It can operate at altitudes more than 18 km for up to 24 hours.

Figure 2.4: Global hawk

2.2.2 LAPs

The LAPs (either aerostats or aerodynes) has the potential of being the best solution into a disaster site and sudden events, however for short period missions. Tethered aerostat as shown in Figure 2.5 [5] can carry large payloads and it is very successful for providing power and communications backhaul. They can operate at altitudes of up to 5 km. They

[4] Image source: www.nasa.gov/centers/dryden/aircraft/GlobalHawk/index.html.
[5] Image source: http://www.carnetdevol.org/actualite-ballon/aerostat/usArmy.html.

can continuously work for 30 days, then eight hours of maintenance and after that go back up for another 30 days.

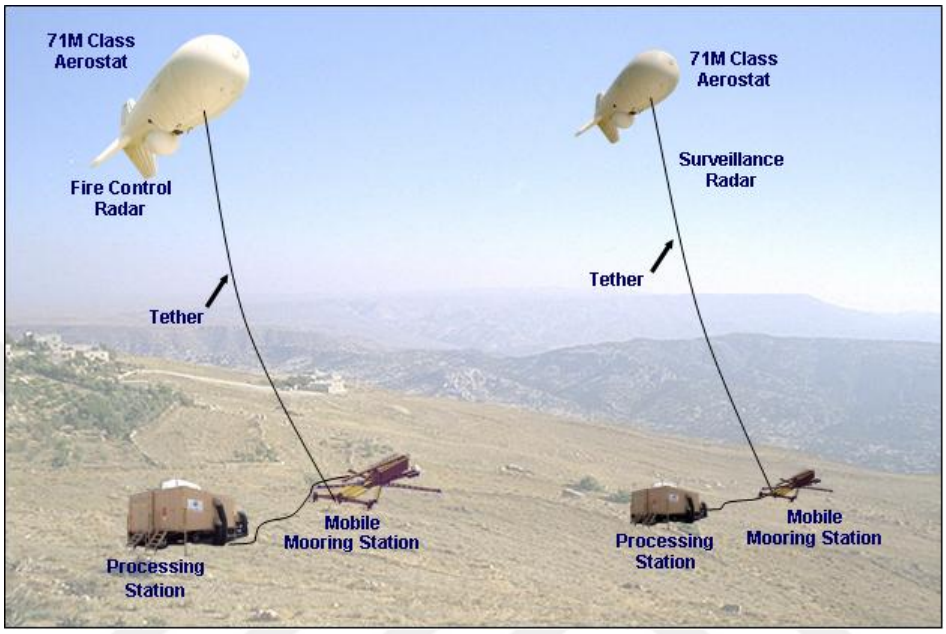

Figure 2.5: Tethered aerostat

Another example is the Hybrid Air Vehicle (unmanned airship) shown in Figure 2.6 [6], which can reach the altitude of 6 km and stay there for up to three weeks. It can be loaded with communications relays, cameras, infrared sensors and other payloads. Also, it can be re-sized to reach to conventionally unreachable areas.

Finally, the Helikite, which is a hybrid kite and tethered aerostat as shown in Figure 2.7 [7], has many reasons for being a promising solution for LAPs. It is a combination of a helium balloon and a kite, that achieve its lift by using both wind and helium. Additionally, it can stay at low altitudes, even with more wind than classical aerostats. It is capable of operating for many weeks without significant support.

[6]Image source: http://www.lindstrandtech.com/
[7]Image source: http://www.allsopp.co.uk/

Figure 2.6: Hybrid air vehicle

2.3 Applications

The ITU recommended that the services and broadband communications from the aerial platforms can be referred to air base stations (ABSs) or flying relays equipped with radio equipment supported by technologies and standards of terrestrial and satellite communication.

Fixed broadband wireless access (FBWA)

FBWA services provide bandwidth allocation with many GHz since they operate at the millimeter wave bands. ITU has specified 47 / 48 GHz and 28 - 31 GHz to HAPs [19]. Since services need wide bandwidth and high capacity, those frequency bands are the most appropriate. For example, for High-Definition Television (HDTV), Multimedia Distribution Service(MDS), high-speed Internet [20].

Mobile cellular services

The ITU suggested HAPs as an infrastructure for IMT-2000 service with minimal network infrastructure to provide mobile cellular and broadband services. IMT-2000 standard conducted studies on challenges such as cell planning, interference mitigation, and antenna design development. Services based on standards such as Global System Mobile (GSM),

Figure 2.7: Helikite

General Packet Radio service system (GPRS), WCDMA based IMT-2000, CDMA-based UMTS, HSDPA and Wi-MAX from HAPs to provide 3G - 3.75G services have been studied in [21, 22].

Fourth generation (4G) technologies have been investigated using HAPs and LAPs to support a cost-effective deployment and high-capacity networks. Deploying 4G system by employing HAPs and LAPs has been regarded as the best alternative to the conventional terrestrial based infrastructure [23, 24].

2.4 Characteristics of Aerial Platforms VS. Terrestrial Networks

Each of the aerial platforms and classical terrestrial systems has various unique features. The aerial platforms have the advantages of both satellite and terrestrial communication systems. The characteristics of these networks are shown in Table 2.1.

Table 2.1: Comparison between aerial platforms and terrestrial systems

Points of comparison	Terrestrial	LAPs	HAPs	Satellite-LEO
coverage radius	$1-10$ *km*	$5-15$ *km*	$100-150$ *km*	>500 *km*
delay	low	low	considerable	high
path loss model	typically multi-path fading	LOS-NLOS based	nearly LOS	LOS based (rain attenuation)
power supply	electricity	fuel/solar	fuel/solar	solar
maintenance and upgrade	complex in terms of number of BSs	low complexity in terms of coverage	low complexity in terms of coverage	impossible
cost	high in terms of number of BSs	low	low	high in terms of coverage
deployment complexity	medium	low	low	high
mobility	difficult	easy	easy	difficult

2.5 Projects and Industry Research

Many countries have done considerable efforts in developing and studying LAPs and HAPs applications. They began in the 1980s and were known by the ITU-R as a new category of radio stations. Different projects began studying the potential of using aerial telecommunication platforms. Selected research projects from different parts of the world are listed below:

- **Stationary High Altitude Relay Platform (SHARP)**

SHARP was the first research project of HAPs that started in Canada in 1987 [25]. This project investigated the use of microwave-powered airplanes. It provided telecommunications services within an area up to 600 km in diameter at an altitude of 21 km. SHARP has shown that the technical ability to expand the ultra high frequency (UHF) mobile radio and radiotelephone services along with super high frequency (SHF) direct broadcast TV channels to rural areas provided safe radio telephone service to users.

- **High-Altitude Long Endurance Platform (HALEP)**

The main objective of this project to exploit the HAP utility in emergency cases and disaster situations in Canada. This project provided remote sensing to disaster management and mitigation. HALEP systems operated at altitude of 15 Km and used advanced aircraft or balloon technologies [26].

- **ABSOLUTE project**

"Aerial Base Stations with Opportunistic Links For Unexpected and Temporary Events (ABSOLUTE)" is an EU-funded program that started since 2013. An LTE-A aerial base station (AeNB) by LAPs was designed for providing excellent coverage and high data rate for public safety users during disaster situations [6, 23]. The objective here is to provide safe telecommunication services by LAPs which could be rapidly launched and connected with satellite and terrestrial networks. LAPs were chosen instead of HAPs due to its lower implementation cost and the rapid deployment.

Furthermore, **Facebook** and **Google** are studying the possibility of using ABSs to provide internet access in the whole world. Facebook is working on ways for providing the internet to ground users from the sky through many technologies using high-altitude long-endurance airplanes and satellites [27]. Additionally, the Google Loon project was designed to provide a coverage to remote regions. Loon is a balloon which operates at an altitude of 20 km for covering selected large areas with wireless communications services [28].

Chapter 3

Optimization Of Aerial Base Station Location In LAP In Disaster Situations

3.1 Introduction

Telecommunication networks play a critical supportive role during high-risk events such a disaster recovery and emergency cases, etc. Currently, communication networks, like Public Protection and Disaster Relief (PPDR), are limited in coverage and capacity utilization [29]. Also, they are limited by developing standards and advanced technologies. Basically, in the cellular network, communications depending on fixed infrastructure could be destroyed during disasters such as earthquakes, or tsunamis. Utilizing airborne base station is one of the prospective feasible solutions for realizing communication recovery networks [30].

For disaster situations, emergency networks face tough constraints regarding their total energy consumption. Indeed, the emergency communication network should guarantee energy efficient processes to maximize the disaster areas survivability. Moreover, the energy consumption for the links between ground and LAPs which depends on the quality and the availability of the channel, must be carefully investigated and optimized.

The most relevant work on energy efficiency for aerial cellular networks during disaster scenarios is using cooperative relay schemes. The authors in [31] introduced a cooperative algorithm for uplink and downlink channels by taking into account the relay nodes locations in the environment and selecting the best link which minimizes the overall energy consumption. In [11], the authors considered a cluster of nodes cooperating together and analyzed the corresponding energy efficiency due to cooperation. However, they considered those relays had fixed positions in the air and the best communication link that provided energy efficient depended on the number of relays. Moreover, in [32], the authors proposed path planning procedure for UAV that collected information from a specific area. UAVs' movement path was planned by visiting potential way points, which were optimized by particle swarm optimization depending on energy consumption, bit error rate (BER) and time delay of the UAV. Additionally, in [30], the authors proposed a new scheme that selected the best link based on channel conditions by cooperating between mobile terrestrial devices that improved energy efficiency in the uplink. Finally, in [10], the authors introduced an approach to provide maximum coverage for users on the ground by optimizing the LAP's altitude.

In this chapter, a new algorithm for adapting the position of ABS to support minimum power consumption by minimizing the total pathloss of subscribers is proposed. We assume the knowledge of the users' location in outdoor environments [33]. Additionally, we derive a formula for the outage probability with respect to the shadow fading margin that can measure the performance of our system.

3.2 System Model

Many studies are available in the literature for modelling the air-to-ground (ATG) link. For instance, study [8], introduced a new ATG communication modelling over urban environments for LAP, when the links between aerial platform and ground device were considered as two propagation groups. These groups were proved statistically, where the first group related to LOS receivers, however the second group related to NLOS receivers.

3.2.1 LAP Channel Model

The received power γ_r from the LAP is given by

$$\gamma_r = \begin{cases} \gamma_t + G_t + G_r - PL_{i,LOS} & \text{LOS} \\ \gamma_t + G_t + G_r - PL_{i,NLOS} & \text{NLOS} \end{cases} \tag{3.1}$$

where γ_t, G_t, G_r and PL_i are the transmitted power, the transmitted antenna gain, the received antenna gain and the path loss from the LAP to i_{th} receiver respectively. So we can describe the total path-loss of all users

$$Total\ PL \quad = \quad \sum_i PL_i\ [dB] \tag{3.2}$$

The path-loss consists of free space pathloss (FSPL) and the excessive path-loss component as defined in [8]

$$\eta_i \quad = \quad PL_i - FSPL_i\ [dB] \tag{3.3}$$

where η_i is the excessive path-loss component for each receiver. The free-space component depends only on the distance between the ABS and the receiver and operating frequency, as expressed by

$$FSPL_i \quad = \quad 20\log(d_{LAP_i}) + 20\log(f_{MHz}) - 27.55 \quad [dBm] \tag{3.4}$$

where f_{MHz} is the system center frequency in MHz, and d_{LAP_i} represents the distance between the ABS and the receiver that can be expressed as

$$d_{LAP_i} \quad = \quad \Delta(h_i)/\sin(\theta_i) \tag{3.5}$$

where $\Delta(h_i) = h_{LAP} - h_{Rx_i}$, h_{LAP} is the LAP altitude, h_{RX_i} is the receivers' height and θ_i is elevation angle for a certain receiver. In [8], the authors defined the group occurrence probability as the probability of a certain propagation group that happened at a certain elevation angle, and it was denoted as $p_\theta(\zeta)$, where ζ is the propagation group, which was defined as either LOS (1) or NLOS (2). At a certain elevation angle, the joint probability density function (PDF) of $f_\theta(\eta,\zeta)$ which can be expressed as

$$f_\theta(\eta,\zeta) \quad = \quad f_\theta(\eta \mid \zeta) p_\theta(\zeta) \tag{3.6}$$

Table 3.1: LOS parameters of all environments

	$f_1 = 700\ MHz$		$f_2 = 2000\ MHz$		$f_3 = 5800\ MHz$	
	μ_1	(a_1, b_1)	μ_1	(a_1, b_1)	μ_1	(a_1, b_1)
$Sub-Urban$	0	11.53, 0.06	0.1	11.25, 0.06	0.2	11.04, 0.06
$Urban$	0.6	10.98, 0.05	1	10.39, 0.05	1.2	10.67, 0.05
$Dense-Urban$	1	9.64, 0.04	1.6	8.96, 0.04	1.8	9.21, 0.04
$Highrise-Urban$	1.5	9.16, 0.03	2.6	7.37, 0.03	2.5	7.15, 0.03

Table 3.2: NLOS parameters of all environments

	$f_1 = 700\ MHz$		$f_2 = 2000\ MHz$		$f_3 = 5800\ MHz$	
	μ_2	(a_2, b_2)	μ_2	(a_2, b_2)	μ_2	(a_2, b_2)
$Sub-Urban$	18	26.53,0.03	21	32.17,0.03	24	39.56,0.04
$Urban$	17	23.31,0.03	20	29.6,0.03	23	35.85,0.04
$Dense-Urban$	20	30.83,0.04	23	35.97,0.04	26	40.86,0.04
$Highrise-Urban$	29	32.13,0.03	34	37.08,0.03	41	40.96,0.03

where $f_\theta(\eta \mid \zeta)$ is the conditional PDF of η given ζ. For simplifying the mathematical expression of the propagation group distribution $f_\theta(\eta \mid \zeta)$ the authors used the Gaussian distribution model. Thus, $f_\theta(\eta \mid \zeta)$ can be written as follows

$$f_\theta(\eta \mid \zeta) = \mathcal{N}(\mu_\zeta, \sigma_\zeta^2(\theta)) \tag{3.7}$$

where $\mathcal{N}$ is the Gaussian distribution with a mean of μ_ζ and a standard deviation $\sigma_\zeta(\theta)$. The results from [10] are listed in Tables 3.1, 3.2 that show the μ_ζ for each group. The standard deviation of each group that depend on the elevation angle and a propagation group is

$$\sigma_\zeta(\theta) = a_\zeta \exp\left(-b_\zeta.\theta\right) \tag{3.8}$$

where a_ζ and b_ζ are parameters that were obtained from the curve fitting results that depend on the frequency and environment [10]. The Tables 3.1, 3.2 shows the standard deviation values. The group occurrence probability as a function of the elevation angle is chosen as the follows

$$p_\theta(1) \quad = \quad c(\theta - \theta_0)^d \tag{3.9}$$

Table 3.3: Group occurrence probability parameters of all environments

	$f_1 = 700\ MHz$	$f_2 = 2000\ MHz$	$f_3 = 5800\ MHz$
	(c,d)	(c,d)	(c,d)
$Sub-Urban$	0.77, 0.05	0.76, 0.06	0.75, 0.06
$Urban$	0.63, 0.09	0.6, 0.11	0.56, 0.13
$Dense-Urban$	0.37, 0.21	0.36 , 0.21	0.33, 0.23
$Highrise-Urban$	0.06, 0.58	0.05, 0.61	0.05, 0.64

$$p_\theta(2) = 1 - p_\theta(1) \tag{3.10}$$

where θ_0 is the minimum angle allowed by the model which was determined to be 15^0. The frequency and environment dependent parameters c and d, listed in Table 3.3. $p_\theta(1)$ and $p_\theta(2)$, represent the probabilities of receiving LOS group and NLOS group path-loss profile occurrence probabilities, respectively.

3.2.2 Outage Probability

The outage probability is the probability that the received signal fades below a threshold and is dependent on the network geometric design and shadowing parameters. It also depends on various other factors like the receivers distribution, the MAC scheme, and the models of path-loss and fading. In [34], a fade margin model employing the shadowing model developed for HAP communications was proposed to characterize different types of urban environments. Since the propagation model in LAP is different from HAP, we propose this fade margin model below for LAP. The PDF of the γ_r can be derived as

$$p(\gamma_r) = \begin{cases} \frac{1}{\sqrt{2\pi\sigma^2_{LOS}(\theta)}} \exp\left(-\frac{(\gamma_r-\bar{\gamma}_{r,LOS})^2}{\sigma^2_{LOS}(\theta)}\right) & \text{LOS} \\ \frac{1}{\sqrt{2\pi\sigma^2_{NLOS}(\theta)}} \exp\left(-\frac{(\gamma_r-\bar{\gamma}_{r,NLOS})^2}{\sigma^2_{NLOS}(\theta)}\right) & \text{NLOS} \end{cases} \tag{3.11}$$

$$\bar{\gamma}_{r,LOS} = \gamma_t + G_t - FSPL + G_r - \mu_{LOS} \tag{3.12}$$

$$\bar{\gamma}_{r,NLOS} = \gamma_t + G_t - FSPL + G_r - \mu_{NLOS} \tag{3.13}$$

Let γ_{th} be the minimum received power threshold of the mobile station and M_S be the shadowing fade margin. Then the outage probability P_{out} is given by

For LOS

$$P_{OUT,LOS} = P(\gamma_{r,LOS} \leq \gamma_{th} - M_S) \tag{3.14}$$

$$P_{OUT,LOS} = 1 - \int_{\gamma_{th}-M_S}^{\infty} \frac{1}{\sqrt{2\pi\sigma_{LOS}^2(\theta)}} \exp\left(-\frac{(\gamma_{r,LOS} - \bar{\gamma}_{r,LOS})^2}{\sigma_{LOS}^2(\theta)}\right) d\gamma_r \tag{3.15}$$

$$P_{OUT,LOS} = Q\left(\frac{\gamma_{th} - M_S - \bar{\gamma}_{r,LOS}}{\sigma_{LOS}(\theta)}\right) \tag{3.16}$$

For NLOS

$$P_{OUT,NLOS} = P(\gamma_{r,NLOS} \leq \gamma_{th} - M_S) \tag{3.17}$$

$$P_{OUT,NLOS} = 1 - \int_{\gamma_{th}-M_S}^{\infty} \frac{1}{\sqrt{2\pi\sigma_{NLOS}^2(\theta)}} \exp\left(-\frac{(\gamma_{r,NLOS} - \bar{\gamma}_{r,NLOS})^2}{\sigma_{NLOS}^2(\theta)}\right) d\gamma_r \tag{3.18}$$

$$P_{OUT,NLOS} = Q\left(\frac{\gamma_{th} - M_S - \bar{\gamma}_{r,NLOS}}{\sigma_{NLOS}(\theta)}\right) \tag{3.19}$$

So the conclusion is shadowing margin as

$$M_S = \begin{cases} Q^{-1}(P_{OUT})\sigma_{LOS}(\theta) - \gamma_{th} + \bar{\gamma}_{r,LOS} & \text{LOS} \\ Q^{-1}(P_{OUT})\sigma_{NLOS}(\theta) - \gamma_{th} + \bar{\gamma}_{r,NLOS} & \text{NLOS} \end{cases} \tag{3.20}$$

From (20) it can be seen that the M_S is dependent on the elevation angle in the LOS and NLOS scenarios. We derived this formula theoretically so we can use it as a metric to compare the performance of our algorithm depending on the outage probability of the users in normal conditions where ABS location assignment is based on coverage areas.

3.3 ABS Positioning Algorithm

Algorithm 1 ABS Location Optimization Algorithm

procedure AT THE ABS
    Start.
    Find position of each user (x_i, y_i) and find their elevation angles θ_i .
    Start position for $ABS = (X', Y')$ where $X' = mean(x_i)$, $Y' = mean(y_i)$.
    Calculate Total FSPL at this position for all users.
    Using the Urban Statistical Parameters, we decide on the threshold of excessive pathloss probability and get the corresponding allowable FSPL increase.
    Calculate max. distance($d_{maxrange}$) corresponding to searching area radius.
    for $i = X' : 1 : X' + d_{maxrange}$, $j = Y' : 1 : Y' + d_{maxrange}$ **do** Measure the RSS at each position.
    end for
    Move ABS to position of minimum total RSS_{min}.
    if the location or the number of users changes. **then** Measure the RSS at the new mid position of users RSS_{mid}.
        New position = At min(RSS_{mid}, RSS_{min})
    end if
end procedure

The proposed algorithm for positioning the ABS relies on achieving minimum total path-loss for all users. Based on the knowledge of users' location the algorithm adjusts the ABS position to minimize (2) when any user changes his position or a new user enters the coverage area as shown in (21).

$$Optimum\ Position = Position\ at\{\min\{Total\ PL\}\} \tag{3.21}$$

First, we minimize the total FSPL by choosing the position of ABS in the midpoint of all users location since it depends on the distance between users and ABS. After that the ABS starts searching for the position that gives minimum total Received Signal Strength (RSS). The searching area is limited by virtual circle centered at the first position. The radius of this circle depends on the maximum value of total FSPL increase that we can tolerate compared to the excessive pathloss added. Hence, depending on the variance of the appropriate channel model, the limit of this circle is chosen such that the probability of the increase in the total FSPL being compensated by the lower excessive pathloss is below a certain chosen threshold. The threshold is chosen depending on the available power and time limitations.

Table 3.4: System parameters

System parameters	
Area	$300 \times 300\ m^2$
Mobile station transmission power(max.)	21 dBm
ABS transmission power(max.)	30 dBm
Mobile/ABS noise figure	8 dB
Platform height	100 m , 1000 m
Users' height	1m
Number of users	100 users
ABS antenna gain	11 dBi
Mobile station antenna gain	Omni (0 dBi)

3.4 Numerical Results

In our simulation a ($300 \times 300\ m^2$) map and two different geographic distributions of users were used. Simulation was done for all of urban environments (i.e. suburban, urban, dense urban and high-rise urban), and for three different operating frequencies (700 MHz, 2,000 MHz and 5,800 MHz). Here, we too different heights of an aerial base station (100 m, 1000 m) into consideration. Other simulation parameters are listed in Table 3.4. We calculated the outage probability for different shadowing fade margin values using our proposed algorithm and compared for normal case (when we put aerial base station in the middle of map depending on the area that aerial base station can cover). For each fade margin value, 1000 iterations with different users location were done. For each iteration we got the outage probability for both cases (LOS, NLOS) averaged over all users.

As shown in Fig. 3.1, the power consumption is reduced when we put ABS at 100 m height, because the fade margin is reduced using our algorithm compared to normal case by a gain within 3-4 dB and for higher of altitudes (1000 m) gain increase because of higher probability of LOS.

As shown in Fig. 3.2, the Poisson distribution of users offers better power consumption of a gain greater than 10 dB. From the literature, the Poisson distribution is a considerable model that can model the users' location especially in disaster and traffic jam scenarios [35].

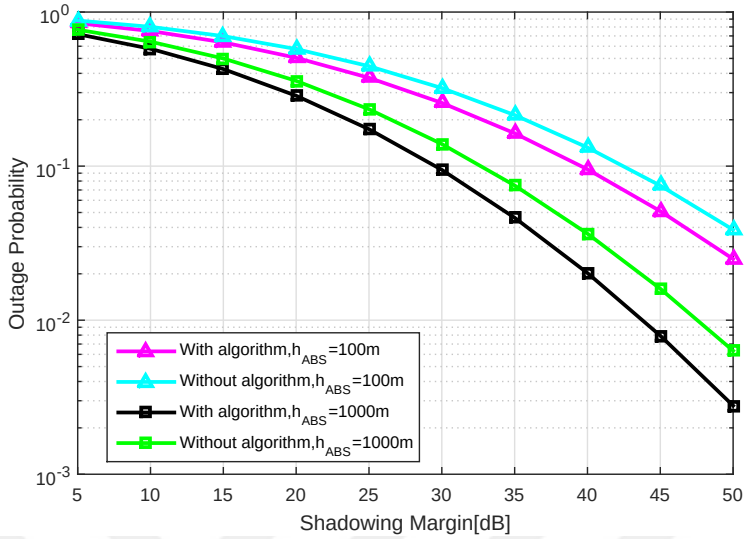

Figure 3.1: Outage probability versus shadowing fade margin, for uniform distribution of users in dense urban area.

3.5 Conclusion

In this chapter, we optimized the location of ABS in LAP to get the minimum total pathloss for all users. We presented a real-time and dynamic algorithm to adapt the location of ABS depending on the channel conditions with respect to energy efficient communications. We derived the outage probability formulas for LOS and NLOS cases. We showed that the employment of this algorithm in ABS system saves more than 10dB in case the users are Poisson distributed.

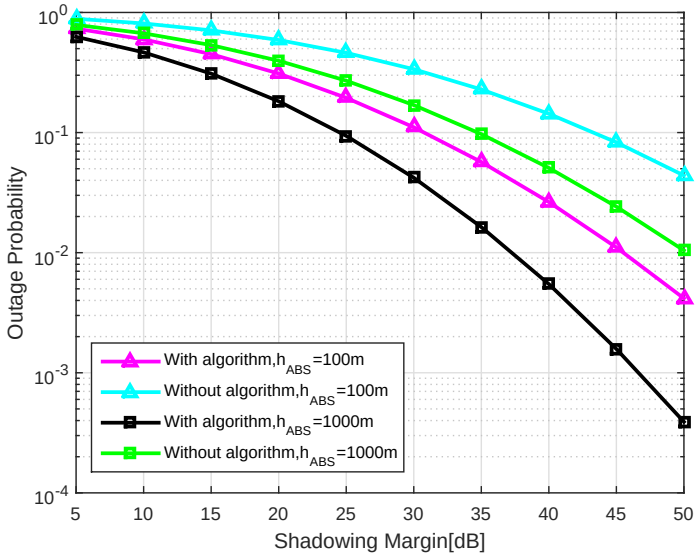

Figure 3.2: Outage probability versus shadowing fade margin, for Poisson distribution of users in dense urban area.

Chapter 4

On Aerial Heterogeneous Cellular Networks: Downlink Coverage Analysis

4.1 Introduction

Future wireless communication systems are expected to provide a massive system capacity, spectral efficiency, more cell throughput and energy efficiency, with respect to existing systems. Furthermore, they should be able to serve a wide variety of users, anytime and anywhere. One of the key concepts to efficiently use the available resources to meet such demands is heterogeneous cellular networks (HCNs) [14].

Due to the big progress in the aerial platforms technology, (i.e. increased carrying capacity, can operate at different altitudes with several tasks, more life time flight, better control management techniques, and the ability to use solar energy), aerial platforms can do multiple tasks such as surveillance, positioning and cellular networks [1]. Also, due to fast deployment, they can scatter in the disaster areas within minimum duration [2]. Aerial telecommunication platforms (ATPs) have been recently studied for future wireless communication services. Many types of aerostats or aerodynes aerial platforms, such as quad-copters, airships, balloons, and UAVs are proposed to be deployed as aerial base stations (ABSs), either in low or high altitudes [1, 12].

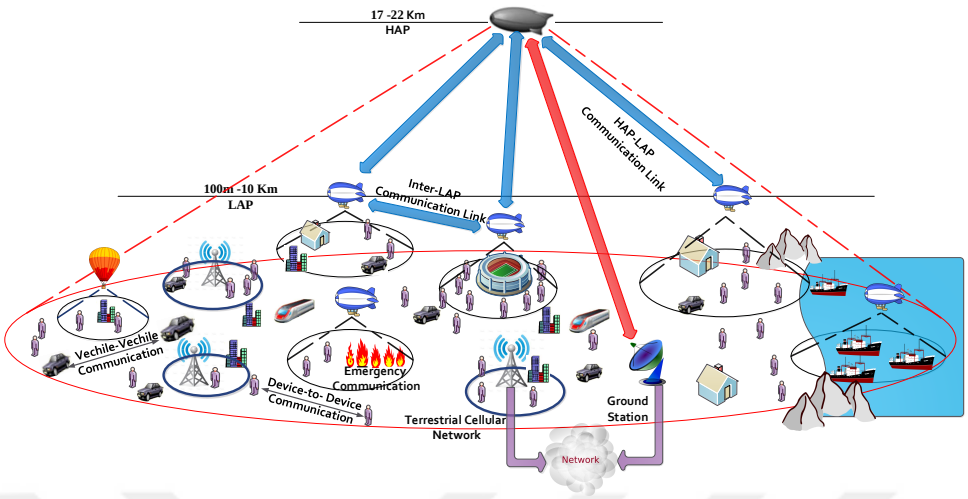

Figure 4.1: Proposed aerial heterogeneous wireless cellular architecture (HAP and LAP Heterogeneous Network)

A multi-tier aerial cellular network architecture, called aerial heterogeneous cellular network (AHCN), is depicted in Fig. 4.1, meeting the needs of connectivity wherever, whenever, and however required.

Obviously, AHCN would be promising to meet the demands of future wireless communication systems. However, incorporating the aerial platforms in a heterogeneous network fashion is not well studied in the literature so far. In particular, analytical evaluations of such coexistence in terms of various performance metrics, e.g., grade of service and overall throughput, is not comprehensively investigated in the current state-of-the-art. This is very critical, because establishing an ABS based cellular network introduces new challenges compared to the classical cellular networks. First, the channel model between the ABS and the ground users will no longer be a classical fading channel [1], [8], [9]. Secondly, unlike conventional fixed BSs, the adjustable height of the ABSs and the interference correlation between them impact the channel characteristics and the coverage performance [10], [36].

Coverage probability is an important metric for performance evaluation of terrestrial cellular systems, which is related to the signal to interference ratio (SIR). For instance, in [37], the authors proposed closed form expressions, which allowed to analytically find the optimal height for a single ABS that maximizes the power and rate gains versus a terrestrial base station. However, interference from neighboring ABSs and shadowing effect were not

taken into account. In [38], the authors derived the coverage probability as a function of the antenna gain without considering the interference coming from different layers. Using circle packing theory, they maximized the coverage in a geographical area which needed to be covered by multiple UAVs. However, those ABSs were at the same altitude and cells did not overlap. In [39], the authors derived an expression for the coverage probability of the target-Rx located on the ground using UAV base stations distributed as a uniform binomial point process. However, while they considered a dominant interferer from the same platform, the shadowing correlation due to collocated obstacles was not taken into account.

The effect of shadowing correlation is significant in obtaining more realistic channel propagation models, which is lacking in the current state of the art for aerial communications platforms. On the other hand, previous work in terrestrial cellular networks show that shadowing correlation significantly affects handover behaviour, interference power and the performance of diversity schemes [36, 40].

The main contributions of this chapter are as follows:

- An AHCN architecture is introduced.

- A framework for SIR analysis for AHCNs is proposed in the cases where, either the downlink channels are correlated or uncorrelated with respect to shadowing.

4.2 Correlated Shadowing Model

In this section, we focus on the effect of correlated shadowing by studying the joint interference distribution with respect to shadowing correlation due to collocated obstacles inside the environment. A reasonable tractable expression for coverage probability that includes correlated shadowing is demonstrated. We assume that the coverage area is one HAP cell overlapped with multiple LAP cells as a circular geographical area of radius R_H and R_L, respectively. Each platform possesses its own path loss exponent α_H, α_L, transmit

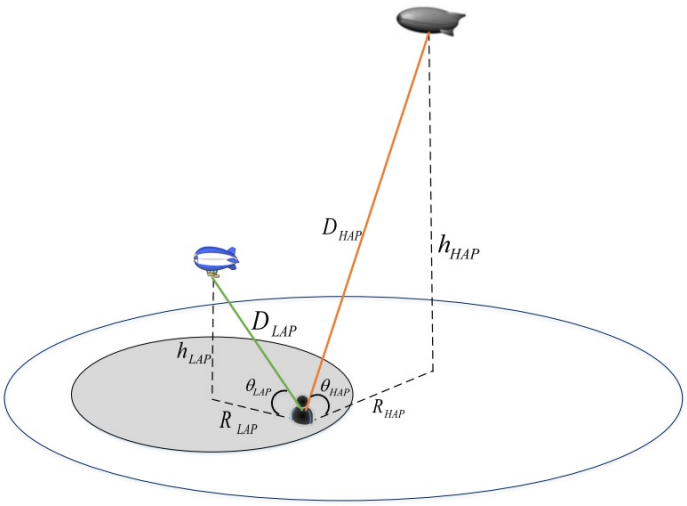

Figure 4.2: System Model

power P_{t_H}, P_{t_L}, altitude h_H, h_L and elevation angle for a target receiver θ_H, θ_L as shown in Fig. 4.2

Here, we consider a shadowing effect on the ATG propagation over urban environments for HAP and LAP, since this propagation model is investigated in [8, 9], where the authors pointed out that ATG communications occurred in two propagation groups. The first group related to LOS receivers, whereas the second group generally corresponded to NLOS receivers. They were a function of the environment, building density and heights, and elevation angles. According to the LOS or NLOS connection between the target receiver and an ABS, the general received signal power γ_r is given by [9]

$$\gamma_r(dB) = \begin{cases} P_t - L - \zeta_{LOS} & \text{for LOS,} \\ P_t - L - \zeta_{NLOS} & \text{for NLOS,} \end{cases} \tag{4.1}$$

where, P_t is the platform transmit power, and L is the path loss which is

$$L = 10\alpha \log\left(\frac{4\pi f_c D_r}{c}\right), \tag{4.2}$$

where f_c is the carrier frequency, c is the speed of light, D_r is the distance between ABS and a target receiver. Also, ζ_{LoS} and ζ_{NLoS} are the shadow fading coefficients with normal distribution on the dB scale for LOS and NLOS links, respectively. The mean μ and variance σ of the shadow fading for LOS and NLOS links are different for each platform. For HAP, $\mu_{H_{LOS}}$ and $\sigma_{H_{LOS}}$ are constants that depend on the environment. However, $\mu_{H_{NLOS}}$

and $\sigma_{H_{NLOS}}$ depend on the elevation angle θ_H and environment parameters [9] as follows

$$\begin{aligned} \mu_{H_{NLOS}}(\theta_H) &= \frac{g_\mu + \theta_H}{h_\mu + i_\mu \theta_H}, \\ \sigma_{H_{NLOS}}(\theta_H) &= \frac{g_\sigma + \theta_H}{h_\sigma + i_\sigma \theta_H}, \end{aligned} \tag{4.3}$$

where, g_μ, h_μ, i_μ, g_σ, h_σ, i_σ are constant empirical parameters for the HAP channel model that depend on the elevation angles range and operating frequency [9]. Similarly, LAP, $\sigma_{L_{LOS}}$ and $\sigma_{L_{NLOS}}$ depend on the elevation angle θ_L and the environment parameters as follows

$$\sigma_{L_{LOS}}(\theta_L) = k_1 e^{\left(-k_2 \theta_L\right)}, \quad \sigma_{L_{NLOS}}(\theta_L) = g_1 e^{\left(-g_2 \theta_L\right)}, \tag{4.4}$$

where k_1, k_2, g_1, g_2 are constant empirical parameters for the LAP channel model that depend on frequency and environment [8]. Moreover, $\mu_{L_{LOS}}$ and $\mu_{L_{NLOS}}$ are constants that depend on the environment [8].

For each target receiver, the PDF of γ_r can be written in a general form as [9]

$$\mathbb{P}(\gamma_r) = \mathbb{P}(\gamma_r | LOS) P_{LOS} + \mathbb{P}(\gamma_r | NLOS) P_{NLOS}, \tag{4.5}$$

where P_{LOS} is the probability of the line of sight, which depends on the environment and the elevation angle of the target receiver in each platform as follows [9], [8]

$$P_{H_{LOS}}(\theta_H) = a - \frac{a-b}{1 + (\frac{\theta_H - n}{d})^e}, \tag{4.6}$$

$$P_{L_{LOS}}(\theta_L) = \tau \Big(\theta_L - 15\Big)^{\upsilon}. \tag{4.7}$$

The constants a, b, n, d, e, τ and υ depend on the environment, and $P_{NLOS}(\theta)$ is the probability of NLOS, where in general $P_{NLOS}(\theta) = 1 - P_{LOS}(\theta)$ for each platform.

4.3 Coverage Analysis of correlated links

The coverage probability is defined as the probability that a target receiver is able to achieve a certain SIR threshold, denoted T, i.e. $\mathbb{P}_{cov} = \mathbb{P}(SIR > T)$. That is, the probability of coverage is the complementary cumulative distribution function (CCDF) of the SIRs over

the network. Our objective in this section is to, analytically, characterize the coverage probability of a single platform in the presence of interference from another platform and the mean interference from the nearest ABS in the same platform of the serving ABS. SIR can be expressed as

$$SIR = \gamma_r - \gamma_I, [dB] \tag{4.8}$$

where γ_I is the total interference which can be expressed as follows

$$\gamma_I = I_H + \bar{I_L}, [dB] \tag{4.9}$$

where I_H is the interference from HAP ABS, and $\bar{I_L}$ is the mean interference from the nearest ABS to the serving ABS in the same tier of LAP and can be expressed as

$$\bar{I_L} = \begin{cases} P_{t_L} - L_L - \mu_{L_{LOS}} & \text{for LOS} \\ P_{t_L} - L_L - \mu_{L_{NLOS}} & \text{for NLOS.} \end{cases} \tag{4.10}$$

We notice that taking the mean interference approximation for the interference from the nearest ABS in the same tier of LAP is a reasonable assumption. Because of the antenna directivity technology, the interference becomes limited [38].

Therefore, every link from the target receiver to every visible ABS is affected by the geometry of the environment, depending on the elevation angle of the visible ABS. We adopt the shadowing correlation model used in [41] in our model. The correlation coefficient is given by the expression

$$\rho = \exp\Big(-\frac{A}{B}\Big(\frac{\Delta\theta}{10}\Big)^2\Big), \tag{4.11}$$

where A and B are the parameters of different environments [41] and $\Delta\theta = \theta_H - \theta_L$ is the elevation separation between the two platforms.

Theorem 1. In case that the paths between the ABSs and a target receiver exhibit a correlated shadowing, the downlink coverage probability for the target receiver served by

the corresponding platform and affected by the interference can be written as follows

$$\begin{aligned}\mathbb{P}_{cov} = {} & P_{LOS_r}P_{LOS_i}\Big(1-Q\Big(\frac{P_{th}+\mu_{LOS_i}-\mu_{LOS_r}}{\sqrt{\sigma^2_{LOS_r}+\sigma^2_{LOS_i}-2\rho\,\sigma_{LOS_r}\sigma_{LOS_i}}}\Big)\Big)\\ & + P_{LOS_r}P_{NLOS_i}\Big(1-Q\Big(\frac{P_{th}+\mu_{NLOS_i}-\mu_{LOS_r}}{\sqrt{\sigma^2_{LOS_r}+\sigma^2_{NLOS_i}-2\rho\,\sigma_{LOS_r}\sigma_{NLOS_i}}}\Big)\Big)\\ & + P_{NLOS_r}P_{LOS_i}\Big(1-Q\Big(\frac{P_{th}+\mu_{LOS_i}-\mu_{NLOS_r}}{\sqrt{\sigma^2_{NLOS_r}+\sigma^2_{LOS_i}-2\rho\,\sigma_{NLOS_r}\sigma_{LOS_i}}}\Big)\Big)\\ & + P_{NLOS_r}P_{NLOS_i}\Big(1-Q\Big(\frac{P_{th}+\mu_{NLOS_i}-\mu_{NLOS_r}}{\sqrt{\sigma^2_{NLOS_r}+\sigma^2_{NLOS_i}-2\rho\,\sigma_{NLOS_r}\sigma_{NLOS_i}}}\Big)\Big).\end{aligned} \tag{4.12}$$

where $Q(\cdot)$ is the Q function and P_{th} is the minimum received power in dB. Note that, $P_{th} = P_{t_r} - L_r - (P_{t_i} - L_i) + \bar{I}_L - T$, where r and i are the indices that refer to received and interference signals, respectively, which are valid for both HAP or LAP, and T is the SIR threshold in dB.

Proof: From (4.1), (4.5) and (4.8) we can write the definition of the coverage probability as

$$\begin{aligned}\mathbb{P}_{cov} &= \mathbb{P}(SIR > T) = \mathbb{P}(\gamma_r - \gamma_i > T)\\ &= P_{LOS_r}P_{LOS_i}\mathbb{P}\Big(\zeta_{LOS_r} - \zeta_{LOS_i} \le P_{th}\Big)\\ &+ P_{LOS_r}P_{NLOS_i}\mathbb{P}\Big(\zeta_{LOS_r} - \zeta_{NLOS_i} \le P_{th}\Big)\\ &+ P_{NLOS_r}P_{LOS_i}\mathbb{P}\Big(\zeta_{NLOS_r} - \zeta_{LOS_i} \le P_{th}\Big)\\ &+ P_{NLOS_r}P_{NLOS_i}\mathbb{P}\Big(\zeta_{NLOS_r} - \zeta_{NLOS_i} \le P_{th}\Big).\end{aligned} \tag{4.13}$$

The probability expressions in (4.13) can be calculated using the property of subtract of two normal distributions [37]. Hence, ζ_{LOS_r} and ζ_{LOS_i} are bi-variate normal distribution with parameters (μ_{LOS_r} and μ_{LOS_i}) and (σ_{LOS_r} and σ_{LOS_i}) and correlation coefficient ρ, we get

$$\begin{aligned}&\mathbb{P}\Big(\zeta_{LOS_r} - \zeta_{LOS_i} \le P_{th}\Big) =\\ &\quad 1 - Q\Big(\frac{P_{th}+\mu_{LOS_i}-\mu_{LOS_r}}{\sqrt{\sigma^2_{LOS_r}+\sigma^2_{LOS_i}-2\rho\,\sigma_{LOS_r}\sigma_{LOS_i}}}\Big).\end{aligned} \tag{4.14}$$

Similarly, the other expressions in (4.12) can be derived in the same way.

From Theorem 1, it is observed that the elevation angle between the ABS (either HAP or LAP) and a target receiver has a significant effect on the coverage by affecting LOS

probability, and the channel parameters. Increasing the ABS altitude leads to higher coverage because of the LOS. However, in the presence of interference, increasing the servicing ABS altitude leads to lower coverage. Furthermore, we can observe an interesting result, namely that the correlation shadowing has a significant effect on the coverage, since increasing this correlation leads to high coverage probability.

4.4 Numerical Results

In this section, we validate the analytical results given in the theorem 1 by comparing them to the simulations results. We assume that the received signal at the user is generated from servicing LAP ABS and the interference signals is from other LAP and the HAP that overlapped with both of them for a given radius $R_H = 30km$. We use the carrier frequency $f_c = 2$ GHz and $\alpha_H = \alpha_L = \alpha = 3.5$ in the dense urban environment. The parameters used in our simulations for the HAP are $P_{t_H} = 60$ dBm, $\mu_{H_{LOS}} = 0$ dB, $\sigma_{H_{LOS}} = 2$ dB. The remaining parameters, $P_{H_{LOS}}$, $\mu_{H_{NLOS}}$ and $\sigma_{H_{NLOS}}$ depend on the elevation angle. The parameters used for the LAP are $P_{t_L} = 30$ dBm, $\mu_{L_{LOS}} = 1.6$ dB and $\mu_{L_{NLOS}} = 23$ dB. Moreover, the parameters $\sigma_{L_{LOS}}$, $\sigma_{L_{NLOS}}$, $P_{H_{LOS}}$ depend on the elevation angle.

Fig. 4.3 compares the coverage probability given by Theorem 1 and by the conventional terrestrial HCN. The gain difference between our proposed AHCN system and the conventional terrestrial HCN system emphasizes the importance and the necessity of our new formula (4.12). In addition, we can observe that the coverage probability in the presence of correlation is higher than that of independent interferers. This can be expected since the correlated interference enhances the coverage of the servicing ABS. However, increasing the LAP altitude reduces the coverage due to the interference from the HAP.

Fig. 4.4 shows the effect of the elevation angles of HAP and LAP on the coverage probability for correlated and uncorrelated links at SIR threshold = 0 dB. It can be observed that as the target receiver gets closer to the servicing ABS, the coverage probability increases for both cases of interferes. However, the gap between the coverage probability of correlated and uncorrelated interferers decreases as the user gets closer to the interfering ABS,

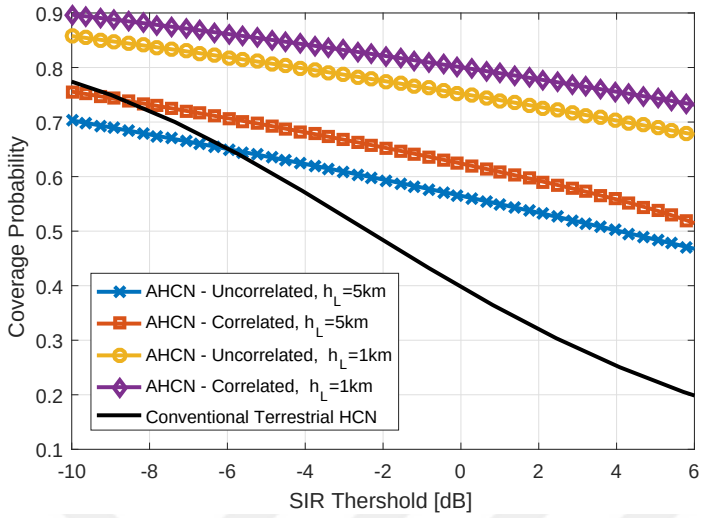

Figure 4.3: Coverage Probability vs. SIR Threshold, $\theta_L = 15^\circ, \theta_H = 20^\circ, h_H = 18km, \rho = 0.9$.

since the interference power increases compared to received signal power.

4.5 Conclusion

In this chapter, we introduced an aerial heterogeneous cellular network structure consisting of static HAPs and LAPs with respect to shadowing environment. We developed an analytical framework for coverage probability to evaluate the AHCN. We noticed that the coverage probability of a single platform in the presence of interference from the same and another platform in AHCNs based on the probabilistic LOS/NLOS links was positively affected by the correlated shadowing fading. This can be used for the antennas at the users for interference cancellation or diversity schemes depending on the availability of the links correlation information. Exploiting this correlation analysis for aerial telecommunications should lead to higher coverage probability.

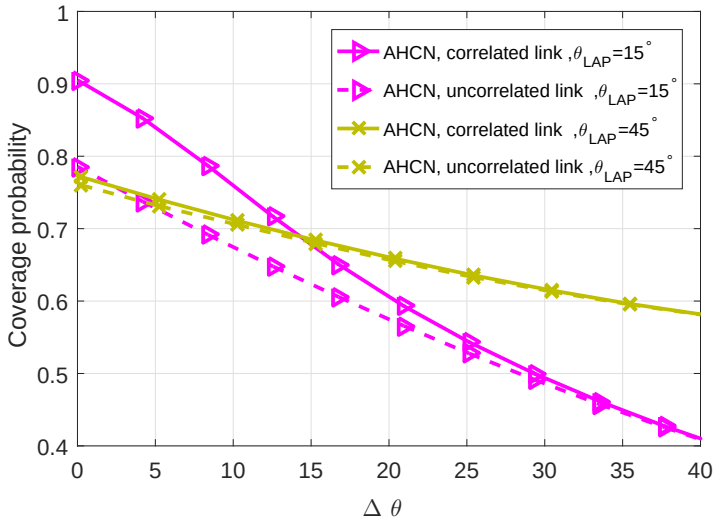

Figure 4.4: Coverage Probability vs. θ_{HAP} and θ_{LAP} with SIR threshold=0 dB, $h_H = 18km, h_L = 1km$.

Chapter 5

Dynamic Utilization of LAPs in Aerial Heterogeneous Cellular Networks

5.1 Introduction

5G systems are expected to provide 1000 times of system capacity, 10 times of spectral efficiency and 25 times of average cell throughput and energy efficiency, compared to existing 4G systems. In addition, they should be able to serve a wide variety of users, anytime and anywhere. One of the key concepts to efficiently use the available resources to meet such demands is HCNs [14]. By coordinating various type of cells, e.g., macro-, micro- and femto- cells, in the same area, HCNs offer a very flexible structure compared to conventional non-heterogeneous systems. Carrying out such a coordination requires considering the transmit powers, coverage areas and spectral resources of different base stations (BSs) and assigning users to the proper BSs based on their requirements. This is usually referred as the user association problem in the literature and plays a critical role in enhancing load balancing, energy and spectrum efficiency in HCNs [15, 16].

Aerial telecommunication platforms (ATPs) have been recently studied for future wireless communication services. Many types of aerostats or aerodynes aerial platforms, such as quad-copters, airships, balloons, and UAVs, are proposed to be deployed as aerial base

stations, either in low or high altitudes [1].

There are many efforts in the literature for developing user association mechanisms, and positioning algorithms considering cell load balancing and outage probability. In [42], the authors introduced a positioning algorithm for UAVs and association of ground users to UAVs in order to meet the quality of service (QoS) and coverage requirements. However, they assumed a single UAV flying over a connected network. In [43], the authors studied the management of core network links connected with dense network of small cells using network flying platforms. They discussed the association problem with constraints on data rate limit, maximum number of links, and bandwidth. In [44], the authors considered several UAVs that relied on the wireless links of the terrestrial network for backhauling. The authors proposed an algorithm for optimizing the locations of UAVs and user-base station association to maximize the sum rate of users. In [45], the authors applied stochastic geometry to model the urban environment effect on the coverage probability of the end user of the UAV network operating at a certain height.

To the best of our knowledge, user-ATP association, cell load, outage probability, and positioning of ABS considering multiple aerial platforms working together as AHCN are not well studied in the literature so far.

In order to unleash the potential benefits of deploying such platforms for cellular communication purposes, we extend our work in chapter 4 to investigate more the AHCN. ABS dynamic placement ability provides the opportunity of having a multi-tier aerial cellular network structure, which is similar to the conventional terrestrial HCN with macro-, pico-, and femto-cells.

The main contributions of this chapter are as follows:

- Using stochastic geometry, the probability that a user is associated with either LAPs or HAP ABS is calculated.
- From the association probability, the cell load of each platform is derived.
- A framework for the outage probability of a typical user for a certain platform is presented, which means the downlink SIR cumulative distribution function.

- An LAP positioning algorithm is proposed to optimize network performance. Based on user location information and the requested peak traffic demand of the users, the algorithm adjusts the ABS positions. Thus, load balancing inside the macro-cell could be enhanced and the usage of spectral resources could be done more efficiently.

5.2 Stochastic geometry model

A generic model of a heterogeneous cellular network should include different layers of BSs. In our model, we assume each layer to be a different aerial platform (HAP or LAP) that is featured by a coverage area, transmit power, and path-loss exponent. In our scenario, an HAP-cell BS network is overlaid with intensive and lower power LAP-cells scenario as seen in Fig. 5.2. The locations of ABSs are modelled according to a uniform point Poisson process (PPP) $\{\Phi_j\}_{j=1,\ldots,K}$ with intensity λ_j for the j^{th} layer (HAPs or LAPs), while the locations of users are modelled according to a homogeneous PPP with intensity λ_N for the N^{th} ABS that is independent of $\{\Phi_j\}_{j=1,\ldots,K}$ [15]. No intra-cell interference is considered, i.e. orthogonal multiple access is employed within each cell. Each platform possesses its own altitude h_j, path loss exponent α_j and allocates the same transmit power P_j for all its ABSs. In the sequel, D_{uj} will denote the distance of the u^{th} user to the nearest ABS in j^{th} layer as shown in Fig. 5.3.

For simplicity, we ignore the fading for the cell association analysis (i.e. the user is associated with the ABS that offers maximum received power averaged over long-term measurement period). Otherwise, the randomness of the channel gain will increase, and subsequently, the outage probability will decrease for the users at the cell edges with low SIR. Furthermore, considering fading may lead to improper handovers (ping-pong effect). Therefore, in cellular networks, the long-term averaged power is typically used for cell association. [15]. Accordingly, the received signal power $\gamma_{u,j}$ by the u^{th} user associated with the strongest ABS_j in terms of long-term averaged power at a distance $D_{u,j}$ is

$$\gamma_{u,j} = P_j |D_{u,j}|^{-\alpha_j}. \tag{5.1}$$

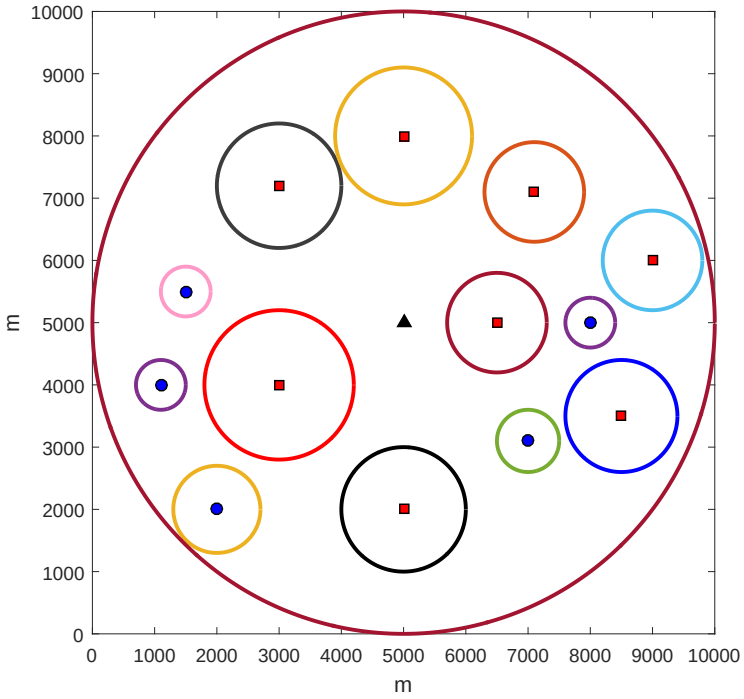

Figure 5.1: An example of downlink AHCN with two tiers of ABSs: Macro drone-cell ABS with high power (black solid triangle) is overlaid with much denser and lower power pico drone-cells (red solid square) or femto drone-cells (blue solid circle).

5.2.1 HAP and LAP association and cell load

Cell association is based on the received power, where each user is associated with the most favourable ABS in terms of maximum received power. We assume that the interference comes from HAP to the LAP associated users and from LAP to the HAP associated users. We define $\tilde{P}_j = \frac{P_j}{P_i}$ and $\tilde{\alpha}_j = \frac{\alpha_j}{\alpha_i}$ as the transmit power ratio and pathloss exponent ratio of interfering layer j to servicing layer i, respectively. Let z be the index of the layer in which the user is associated. The following lemma provides the association probability, which is important for deriving the main results.

Lemma 1. The probability that a user is associated with the i^{th} platform HAPs or LAPs is

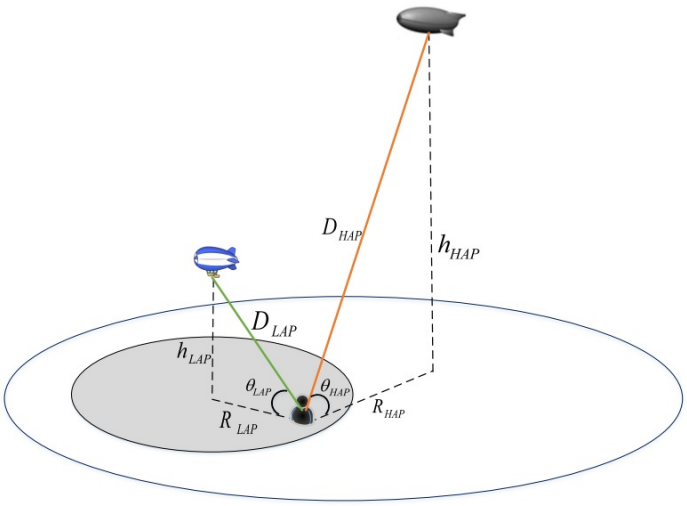

Figure 5.2: System Model

$$P_u(i) = \int_{h_i}^{\infty} \left[2\pi\lambda_i d \exp\{-\pi \sum_{j=1}^{K} \lambda_j (\tilde{P}_j)^{\frac{2}{\alpha_j}} (d^2 - h_i^2)^{\frac{1}{\alpha_j}} \} \right] dd. \tag{5.2}$$

In the case of $\alpha_j = \alpha \; \forall \; j \in \{1, ..., K\}$, the probability can be simplified as

$$P_u(i) = \frac{\lambda_i}{\sum_{j=1, j\neq i}^{K} \lambda_j (\tilde{P}_j)^{\frac{2}{\alpha}} + \lambda_i}. \tag{5.3}$$

Proof: See Appendix A.

From Lemma 1, we can observe that ABSs density, transmit power of the servicing ABSs, and the interfering ABSs are the most effective parameters for assigning the users to the most preferable ABS. However, the altitude of a platform does not affect the user's association. Having determined this probability of user association, we can easily find the average number of users associated with an ABS in the i^{th} platform, which represents the cell load of each platform.

Lemma 2. The cell load of the i^{th} platform is given as

$$U_i = \int_{h_i}^{\infty} \Big[2\pi\lambda_N d \exp\{-\pi \sum_{j=1}^{K} \lambda_j (\tilde{P}_j)^{\frac{2}{\alpha_j}} (d_{ui}^2 - h_i^2)^{\frac{1}{\alpha_j}} \} \Big] dd. \tag{5.4}$$

In the case of $\alpha_j = \alpha \; \forall \; j \in \{1, ..., K\}$, the cell load can be simplified as

$$U_i = \frac{\lambda_N}{\sum\limits_{j=1, j\neq i}^{K} \lambda_j (\tilde{P}_j)^{\frac{2}{\alpha}} + \lambda_i}. \tag{5.5}$$

Proof:

Let N_i is the i^{th} platform users expressed as

$$N_i = P_u(i)\, N_u, \tag{5.6}$$

where N_u is the number of users in the network. We can rewrite (6) as

$$N_i = P_u(i)\, \lambda_N\, A, \tag{5.7}$$

where A is the total serving area. Also we can rewrite the average number of i^{th} platform ABSs, as

$$K_i = \lambda_i\, A, \tag{5.8}$$

Hence the average number of users associated with an ABS in the i^{th} platform is

$$U_i = \frac{N_i}{K_i} = \frac{P_u(i)\, \lambda_N}{\lambda_i}. \tag{5.9}$$

From (5.4) and (5.5) we can notice that, when the ABS density of the i^{th} platform increases, more users are associated with the i^{th} platform but the number of users per ABS decreases.

5.2.2 Statistical distance to the servicing ABS

In this section, we characterize the distribution of the distance between the user and its servicing ABS that will help us in deriving the outage probability. We consider the user at

the origin associated with the i^{th} platform, and X_i as the distance between the user and its servicing ABS.

Lemma 3. The probability density function (PDF) $\mathbf{f}_{X_i}(x)$ of the distance X_i between a typical user at the origin and its servicing ABS is

$$\mathbf{f}_{X_i}(x) = \frac{2\pi\lambda_i}{P_u(i)}\Big[x\exp\{-\pi\sum_{j=1}^{K}\lambda_j(\tilde{P}_j)^{\frac{2}{\alpha_j}}(x^2-h_i^2)^{\frac{1}{\tilde{\alpha}_j}}\}\Big]; \quad \text{for } D_{ui} > x \geq h_i \tag{5.10}$$

Proof: The PDF of X_i is given as

$$\mathbf{f}_{X_i}(x) = \frac{d\mathbf{F}_{X_i}(x)}{dx}, \tag{5.11}$$

$$\mathbf{F}_{X_i}(x) = 1-\mathbb{P}[X_i > x]. \tag{5.12}$$

The probability of $X_i > x$, given the association with the i^{th} platform can be given as

$$\mathbb{P}[X_i > x] = \mathbb{P}[X_i > x | z = i] = \frac{\mathbb{P}[X_i > x, z = i]}{\mathbb{P}[z = i]}, \tag{5.13}$$

where $\mathbb{P}[z=i] = P_u(i)$, and

$$\begin{aligned}\mathbb{P}[X_i > x, z = i] &= \mathbb{P}[X_i > x, \gamma_{u,i} > \max_{j,j\neq i}\gamma_{u,j}] \\ &\overset{(a)}{=} \int_x^{\infty}\Bigg[\prod_{\substack{j=1\\ j\neq i}}^{K}\mathbb{P}[D_{uj} > (\tilde{P}_j)^{\frac{1}{\alpha_j}}D_{ui}^{\frac{1}{\tilde{\alpha}_j}}]\mathbf{f}_{D_{ui}}(d)dd \\ &\overset{(b)}{=} 2\pi\lambda_i\int_x^{\infty}\Big[d\exp\{-\pi\sum_{j=1}^{K}\lambda_j(\tilde{P}_j)^{\frac{2}{\alpha_j}}(d^2-h_i^2)^{\frac{1}{\tilde{\alpha}_j}}\}\Big]dd,\end{aligned} \tag{5.14}$$

where (a) is given by (5.1), and (b) is given from (A.4) and (A.5). By combining (5.14) into (5.13), we get

$$\mathbb{P}[X_i > x] = \frac{2\pi\lambda_i}{P_u(i)}\int_x^{\infty}\Big[d\exp\{-\pi\sum_{j=1}^{K}\lambda_j(\tilde{P}_j)^{\frac{2}{\alpha_j}}(d^2-h_i^2)^{\frac{1}{\tilde{\alpha}_j}}\}\Big]dd, \tag{5.15}$$

From (5.15) and (5.12), we can get the PDF as

$$\mathbf{f}_{X_i}(x) = \frac{2\pi\lambda_i}{P_u(i)}\Big[x\exp\{-\pi\sum_{j=1}^{K}\lambda_j(\tilde{P}_j)^{\frac{2}{\alpha_j}}(x^2-h_i^2)^{\frac{1}{\alpha_j}}\}\Big]; \quad \text{for } D_{ui} > x \geq h_i \tag{5.16}$$

5.3 Outage Probability

In this section, we study the outage probability as the performance metric of our network architecture. We define the outage probability P_{OUT} of the link between a user and its associated ABS as the probability that the instantaneous SIR at a random user's location is less than a certain SIR threshold (i.e. the CDF of SIR over the entire network). The probability is given as

$$P_{OUT} = \sum_{i=1}^{K} P_{OUT}(i)P_u(i), \tag{5.17}$$

where $P_u(i)$ is the platform association probability given in Lemma 1 and $P_{OUT}(i)$ is the outage probability of a typical user associated with i^{th} platform. For a certain SIR and an $SIR_i(x)$ of a typical user at a distance x from its servicing ABS, the outage probability is

$$P_{OUT}(i) = \mathbb{E}_{X_i}[\mathbb{P}[SIR_i(x) \leq T]], \tag{5.18}$$

Note that the outage probability averaged over the coverage area defined by $\mathbf{f}_{X_i}(x)$ in Lemma 3.

The SIR of the u^{th} user at a random distance x from its associated ABS in platform i is

$$SIR_i(x) = \frac{P_i q_{i,u}|x|^{-\alpha_i}}{\sum_{\substack{j=1 \\ j\neq i}}^{K} P_j q_{j,u}|D_{u,j}|^{-\alpha_j}}, \tag{5.19}$$

where $q_{i,u}$ and $q_{j,u}$ are random variables with the exponential distribution channel power for servicing and interfering ABSs, respectively.

In the following theorem, we obtain the outage probability for the user located at the origin and served by i^{th} ABS and affected by the j^{th} interfere ABS.

Theorem 2. *The outage probability of a typical user associated with the i^{th} platform is*

$$P_{OUT}(i) = 1 - \frac{2\pi\lambda_i}{P_u(i)} \int_{h_i}^{D_{u,i}} \Big[x \exp\{-\pi \sum_{j=1 j\neq i}^{K} \lambda_j \mathbb{W}_j\} \Big] dx, \tag{5.20}$$

where

$$\mathbb{W}_j = (\tilde{P}_j)^{\frac{2}{\alpha_j}} (x^2 - h_i^2)^{\frac{1}{\alpha_j}} + \mathbb{A}(\alpha_j, T),$$

and

$$\mathbb{A}(\alpha_j, T) = \frac{2\, T^{\frac{-2}{\alpha_j}+1}}{\alpha_j - 2} {}_2\mathrm{F}_1[1, 1 - \frac{2}{\alpha_j}; 2 - \frac{2}{\alpha_j}; -T].$$

Proof: See Appendix A.

Even though theorem 2 does not give a simple expression, we can compute the integral numerically. In the following corollary, we obtain a closed-form for special case.

Corollary: The outage probability of the i^{th} platform and overall in case $\{\alpha_j\} = \alpha$ is

$$P_{OUT}(i) = 1 - \frac{e^{\mathbb{A}(\alpha,T))} (e^{-\pi(D_i - h_i)(D_i + h_i) \sum_{j=1, j\neq i}^{K} \lambda_j (\tilde{P}_j)^{\frac{2}{\alpha}}} - 1)}{P_u(i) \sum_{j=1, j\neq i}^{K} \lambda_j (\tilde{P}_j)^{\frac{2}{\alpha}}}. \tag{5.21}$$

Proof: In the case $\{\alpha_j\} = \alpha$, we can rewrite (5.20) as

$$\begin{aligned} P_{OUT}(i) &= 1 - \frac{2\pi\lambda_i}{P_u(i)} \int_{h_i}^{D_{u,i}} \Big[x \exp\{-\pi \sum_{j=1, j\neq i}^{K} \lambda_j (\tilde{P}_j)^{\frac{2}{\alpha}} \\ &(x^2 - h_i^2) + [\frac{2\, T^{\frac{-2}{\alpha}+1}}{\alpha - 2} {}_2\mathrm{F}_1[1, 1 - \frac{2}{\alpha}; 2 - \frac{2}{\alpha}; -T]]\} \Big] dx \\ &= 1 - \frac{2\pi\lambda_i}{P_u(i)} \int_{h_i}^{D_{u,i}} x \exp\{-\pi(x^2 - h_i^2)(\sum_{j=1, j\neq i}^{K} \lambda_j (\tilde{P}_j)^{\frac{2}{\alpha}} \\ &\qquad + \mathbb{A}(\alpha, T))\}. \end{aligned} \tag{5.22}$$

By applying the change of variables we will get the result in (5.21).

This closed-form expression is straightforward and much simpler. Also, we can observe that the outage probability depends on the transmit powers and the densities of the ABSs of servicing and interference platforms. Furthermore, altitude of the servicing platform impacts the outage which can be optimized to satisfy the QoS requirements. In the following section, we present an algorithm to find the optimum positions for LAPs in AHCN depending on users' demands and locations in order to minimize the ABS's load and provide users with high QoS.

5.4 Proposed LAPs Positioning Algorithm

In this section, we propose an algorithm for positioning the LAPs in AHCN to achieve load balancing based on the knowledge of users' locations and the requested peak traffic demand of the users (users' demands). The algorithm adjusts the LAPs' positions to achieve load balancing for the entire network (i.e HAP and LAPs) and enhances the QoS of users. In our algorithm, we focus on the cell load from the users' demands and ABSs capacity perspective.

We assume that users arrive uniformly on the network and random data rate demands are required. The arrival times and demands are assumed to be independent among users. We assume the existence of a space-time Poisson process of arrival, where the users do not move during their service. Each user in the system stays for a random period of time

because the users' demands depend on the other users served by the same base station [35].

First, we will introduce the main algorithm used for coordination between HAP and LAPs. Then, we explain in detail the LAPs positioning algorithm. In our algorithm, we assume the coexistence of one HAP and multiple LAPs to build a heterogeneous network. Fig. 5.4 and Fig. 5.5 show a simulated example of applying our algorithm using four LAPs and a single HAP to simplify the idea of our algorithm. As shown in both algorithms,

Algorithm 2 Main Algorithm

1: Define ABS_{HAP} location (X_{HAP_0}, Y_{HAP_0}, Z_{HAP_0}).
2: Define $LAPs$ locations (X_{LAP_j}, Y_{LAP_j}, Z_{LAP_j}), $j = 1,..,K$, where K is the number of LAPs.
3: Find all user locations in HAP coverage area (x_u, y_u), $u = 1,..,N$, where u is user index and N is the total number of users in the HAP area.
4: Define how many users in the HAP coverage area are associated to each LAP cell ($U_j = N_j$, $U_{HAP} = N - \sum_j U_j$), where N_j is the maximum number of users in the j^{th} LAP coverage area.
5: Define the maximum load of each ABS (C_j, C_{HAP}).
6: Find the rate demand of the associated users in each cell ($R_j = \sum_u^{U_j} R_u$, $R_{HAP} = \sum_u^{U_{HAP}} R_u$).
7: **for** j=1,..,k **do**
8: **if** $R_j > C_j$ **then** run Algorithm 2 to change the LAP_j location to achieve load balancing and increase QoS.
9: Calculate $U_j^{new} = U_j - U_j^{out}$, where U_j^{out} is the number of users that will be removed from ABS_j coverage area after the positioning process.
10: Calculate $U_{HAP}^{new} = U_{HAP} + \sum U_j^{out}$.
11: **end if**
12: **end for**

the update of users' locations and demands depends on how frequent the load exceeds the maximum load capacity of the cell.

5.5 Numerical Results

In this section we verify the validity of our findings and evaluate our algorithm using simulations. We consider two scenarios: 1) To verify the analysis, the first scenario assumes a

Algorithm 3 ABS Location Optimization Algorithm

1: Sort the vector of rate demands $R_s = [R_1, R_2, ..., R_{N_j}]$ in descending order in the j^{th} LAP coverage area. Sort also the corresponding locations (X_s, Y_s)=$[(X_1, Y_1), (X_2, Y_2), ..., (X_{U_j}, Y_{U_j})]$.
2: Define R_m as the user rate accumulator, initialized as 0 and define i as a counter initialized as 0.
3: **while** $C_j > R_m$ **do**
4: $\quad i = i + 1$.
5: $\quad R_m = R_m + R_i$.
6: **end while**
7: $ABS_j^{location} = mean((X_1, X_2, ...X_i), (Y_1, Y_2, ...Y_i))$.
8: Calculate the optimum altitude z_j according to [10].

network in which both the HAP and the LAPs are static. 2) To evaluate our algorithm, the second scenario assumes a network in which the HAP is static and LAPs are dynamic and moving according to the algorithm for balancing the traffic load.

5.5.1 Performance of the outage model

In order to verify our findings on the outage probabilities in the static scenario, we performed Monte Carlo simulations where a (10000 $m \times 10000$ m) area is covered with ABSs deployed following the given model.

The simulation results have been averaged over 10000 network realization, where for each ABS location update, we find the outage probabilities of the user located at the origin of our map. Other simulation parameters, listed in Table 5.I. Fig. 5.6, compare the proposed outage probability model of the AHCN with the conventional terrestrial HCN in [15]. Since AHCN consists of HAP and LAP cells modelled based on a PPP deployment, and the conventional HCN consists of macro- and pico- cells modelled according to a PPP deployment as well. From Fig. 5.6, we can observe that the analytic results given in (20) are almost as precise as the simulated ones for all SIR thresholds in the two cases (either HAP is the servicing ABS or LAP is the servicing ABS). Moreover, we can observe that the outage probability of AHCN in the case when the LAP is the servicing ABS is

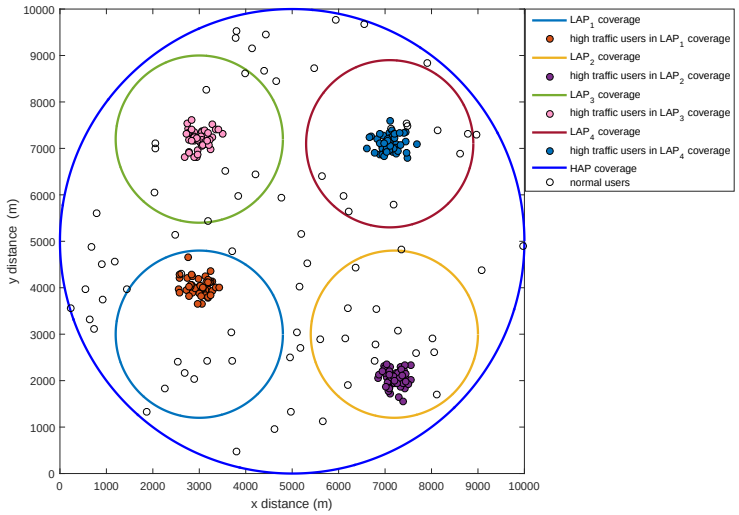

Figure 5.3: Illustration of HAP- and LAPs- based heterogeneous network with high traffic load before applying Algorithm 1 and 2.

significantly less than the outage probability of the conventional HCN. This gain emphasizes the necessity of our proposed formula in (20). However, in the case when the HAP is the servicing ABS, the outage probability is higher than the conventional HCN for lower SIR thresholds. This occurs due to the long distance between the HAP and the user, since the user connects to the ABS with the maximum received power. However, at high SIR thresholds, the effect of the long distance does not appear.

Fig. 5.7 shows the number of ABSs effect in both cases when either the HAP or the LAP is the servicing ABS with different path-loss exponent. From Fig. 5.7, we observe that when the LAP experiences higher path-loss exponent, the outage is significantly better than when the HAP experiences higher path-loss exponent. Intuitively, the interference between the LAP and the HAP decreases with high path-loss so the LAP is more isolated from the HAP cell. We conclude here that employing ABSs in an area with higher path-loss is better.

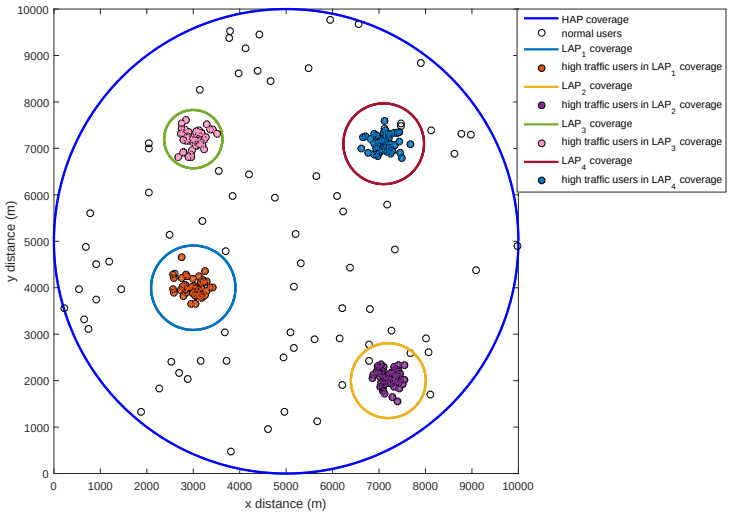

Figure 5.4: Illustration of HAP- and LAPs- based heterogeneous network with high traffic load after applying Algorithm 1 and 2.

5.5.2 Utilization of the positioning algorithm

In order to verify our algorithm, we compare the performance of the static and dynamic scenarios (i.e. using the positioning algorithm) via investigating the utilization of the ABSs and the user outage probability. First, we calculate the ABS' utilization for different maximum load values where ABS' utilization is defined as the probability of having greater users' demand than the ABS' maximum load. We consider that the number of LAPs in this case is equal to four.

In Fig. 5.8, the ABS' utilization for the dynamic and static cases are compared. In static case we assume equal coverage area for all LAPs, while the dynamic case corresponds to the usage of our algorithm. It is shown that our dynamic localization method requires much lower ABS' utilization for a given maximum load compared to the static case by optimally locating LAPs within the coverage of HAP. Thus, the overall system capacity could be enhanced significantly.

We also evaluate the proposed algorithm performance via the comparison of user outage

Table 5.1: Simulation parameters

Simulation parameters	
HAP ABS max. transmission power	40 dBm
LAP ABS max. transmission power	30 dBm
HAP altitude	18 km
LAP altitude	1 km
Path loss exponent	3
Max. number of users in a cell	1000
System bandwidth	1.4 MHz

probabilities for static and proposed dynamic cases. We consider a simple scenario where each user in the AHCN is served by being assigned to any available channel corresponds to a spectral resource with a fixed bandwidth. User outage probability (also called blockage probability) is defined as the probability of providing no service to a user due to the non-availability of channels in the corresponding cell. Since we propose a heterogeneous cellular structure including LAP cells inside a HAP cell, available channels are shared between both of them. We also assume that LAPs cells are using the same channels, i.e. the frequency reuse factor is one for all LAPs cells. Note that our evaluation criteria here are based on a grade-of-service point of view [37] rather than considering link capacities, and therefore, co-channel interference type of factors affecting the service quality are not included. The total number of channels is specified as 140 for this simulation. We deployed different number of LAPs in an HAP's coverage area and the number of channels assigned for each LAP is determined as 12. Note that the same 12 channels are assigned to all the LAPs in a frequency reuse fashion. Therefore, the remaining 128 channels can be utilized for the users served by the HAP.

As shown in Fig. 5.9, the dynamic usage of LAPs significantly improves the load balancing by decreasing the user outage probability. For example, when 200 users are requesting service in the HAP area, user outage probability is very close to zero when 6 LAPs are dynamically used. This means that the HAP almost never needs to serve more than 128 users, since dynamic LAPs are able to serve at least 72 users by adjusting their positions

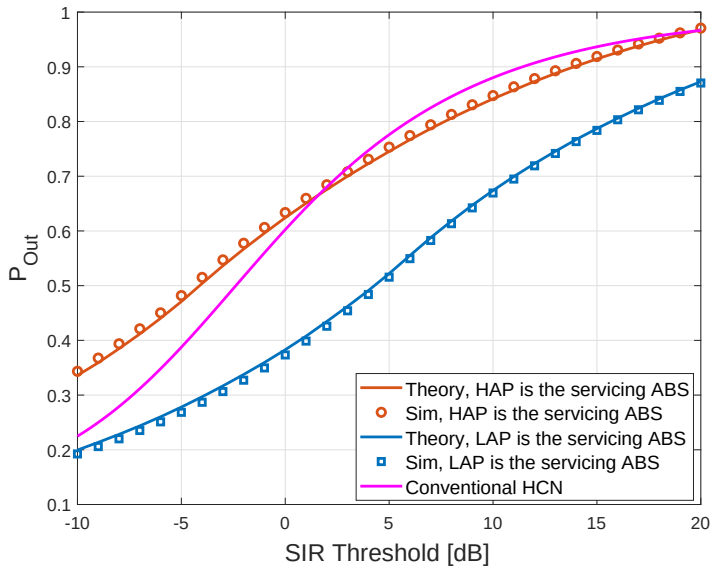

Figure 5.5: Outage probability of the servicing ABSs in a two-tier AHCN, ($\lambda_i = 2\lambda_n$)

properly. On the other hand, approximately 23% of the users cannot get service for the static usage of LAPs. This is because many of the LAPs are not able to have enough number of users in their coverage areas due to the fixed positioning. Therefore, the number of users who must be served by the HAP increases and the 128 channels managed by the HAP are not sufficient to serve them all.

5.6 Conclusion

In this chapter, we introduced an aerial heterogeneous cellular network structure consisting of HAPs and dynamically deployed LAPs with respect to stochastic geometry environment. We deduced the corresponding association probability that helped us calculate the cell load with an ABS in each platform. Then we developed a new analytical framework to evaluate the outage probability performance in such network. It is interesting to notice that the altitudes of the interfering platforms do not affect the outage probability, however the number of interfering platforms and their densities affect the outage probability. This

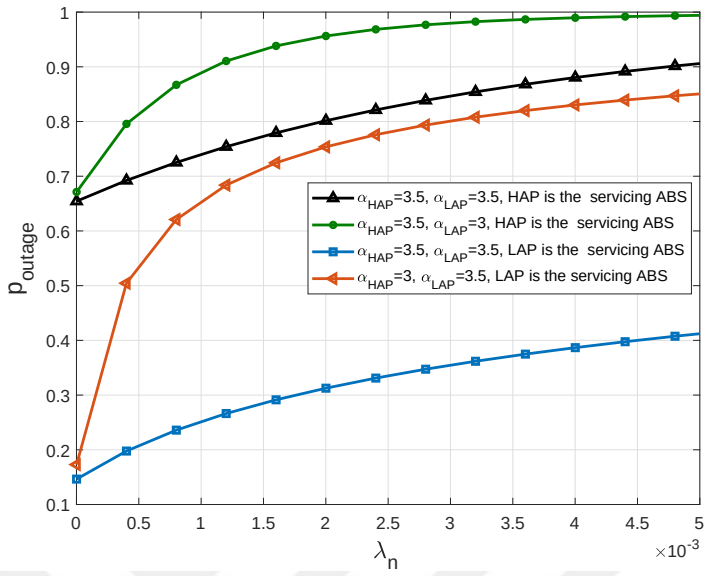

Figure 5.6: Outage probability versus the density of the interfering cells in a two-tier AHCN with SIR threshold=0 dB, $\lambda_i = 0.001$.

means that even randomly adding more LAP cells to a network for coverage improvement does not necessarily reduce the performance of the overall network. Subsequently, we proposed an algorithm for positioning the LAPs in order to achieve load balancing and increase throughput in such network. Simulation results showed that, compared to the static case, dynamic positioning of LAPs provides efficient usage of ABSs resources and enhances the service quality for users in high traffic scenarios.

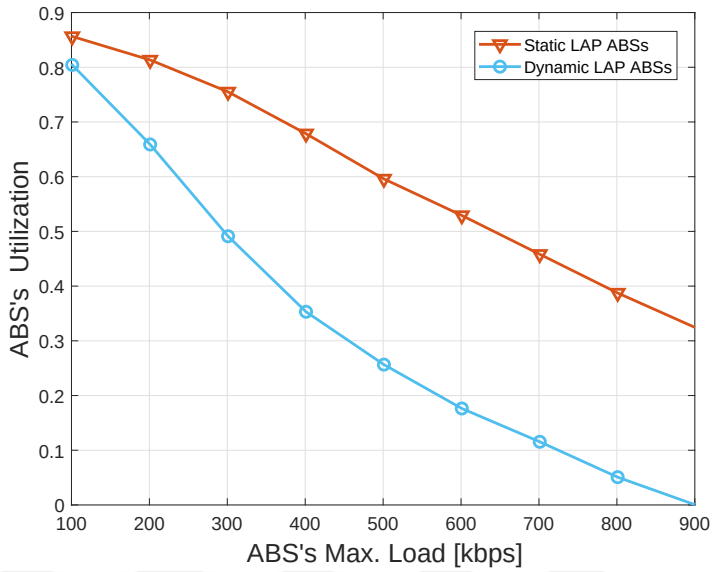

Figure 5.7: ABS's utilization verses ABS's load for static and moving ABSs in the LAP.

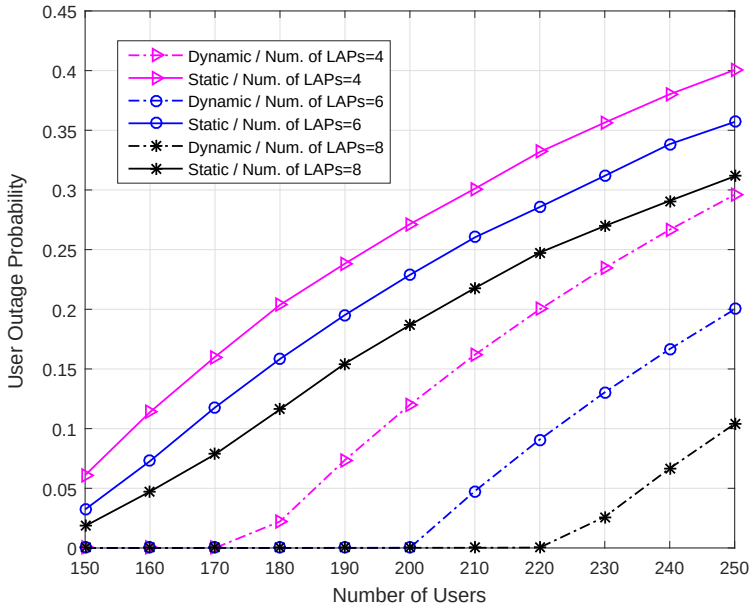

Figure 5.8: User outage probabilities for dynamic and static usage of LAPs versus different number of users.

Chapter 6

Concluding Remarks

The rapid increase in the demand for broadband wireless communications has led to the rapid evolution of the conventional terrestrial and satellite networks. Delivering high data rate, high efficiency, a wide variety of applications and supporting coverage to remote and disaster areas is a challenging task to the next generation wireless systems. Aerial platforms are one of the promising solutions to meet all of those challenges. Taking advantage of the mobility, lower cost and LOS communications of aerial platforms, several techniques and algorithms are developed to meet the next generation's challenges.

In this thesis, an overview was given describing the importance and availability of the aerial platforms for the next generation of wireless communication. Also, we proposed an algorithm that utilized the ABS's mobility in LAP. By controlling the location of ABSs in LAPs, we introduced an algorithm to minimize the power consumption due to path loss. An algorithm attempting to maximize the received power at ABS by moving the ABS between multiple points within its whole coverage was developed. The employment of this algorithm saved more than 10 dB per user in case of Poisson distributed users.
Furthermore, the coexistence performance of heterogeneous aerial platforms (HAP, LAPs) systems was investigated. We provided an analytical framework for evaluating the coverage probability of such system based on the LOS/NLOS links with respect to the shadow

fading effect. We also showed the impact of correlated interferers platforms on the coverage probability. The positive effect of the correlated interferers could be useful for the antennas at the users for interference cancellation or diversity schemes depending on the availability of the links correlation information. Exploiting this correlation analysis for aerial telecommunications should lead to higher coverage probability.

Finally, we completed our work by deriving the association probability for the serviced users in AHCN. This helped us calculate the cell load with an ABS in each platform. Then we developed a new analytical framework to evaluate the outage probability performance in such network. It is interesting to note that the altitudes of the interfering platforms do not affect the outage probability. However, the number of interfering platforms and their densities affect the outage probability. This means that even randomly adding more LAP cells to a network for coverage improvement does not necessarily reduce the performance of the overall network. Subsequently, we have proposed an algorithm for positioning the LAPs in order to achieve load balancing and increase throughput in such network. Simulation results showed that, compared to the static case, dynamic positioning of LAPs provided efficient usage of ABSs resources and enhanced the service quality for users in high traffic scenarios.

Bibliography

[1] C. Sathyanarayanan, K. Gomez, A. Al-Hourani, K. Sithamparanathan, T. Rasheed, L. Goratti, L. Reynaud, D. Grace, I. Bucaille, T. Wirth, *et al.*, "Designing and Implementing Future Aerial Communication Networks," *IEEE Communications Magazine*, 2016.

[2] S. Kandeepan, K. Gomez, L. Reynaud, and T. Rasheed, "Aerial-Terrestrial Communications: Terrestrial Cooperation And Energy-Efficient Transmissions To Aerial Base Stations," *IEEE Transactions on Aerospace and Electronic Systems*, vol. 50, no. 4, pp. 2715–2735, 2014.

[3] M. M. Nia and T. A. Rahman, "High Altitude Platform System (HAPS) And Co-existence With Fixed Satellite Service (FSS) In Frequency Range 5850–7075 MHz," in *Wireless Communication, Vehicular Technology, Information Theory and Aerospace & Electronic Systems Technology (Wireless VITAE), 2011 2nd International Conference on*, pp. 1–6, IEEE, 2011.

[4] K. Gomez, T. Rasheed, L. Reynaud, and S. Kandeepan, "On The Performance Of Aerial LTE Base-Stations For Public Safety And Emergency Recovery," in *Globecom Workshops (GC Wkshps), 2013 IEEE*, pp. 1391–1396, IEEE, 2013.

[5] S. H. Alnajjar, F. Malek, M. S. Razalli, and M. S. Ahmad, "Low-Altitude Platform to Enhance Communications Reliability in Disaster Environments," *Journal of Advances in Information Technology*, vol. 5, no. 1, pp. 21–30, 2014.

[6] E. I. I. Project, "ABSOLUTE." `http://www.absoluteproject.eu/reports/publications`, 2013.

[7] A. Al-Hourani and S. Kandeepan, "Cognitive Relay Nodes For Airborne LTE Emergency Networks," in *Signal Processing and Communication Systems (ICSPCS), 2013 7th International Conference on*, pp. 1–9, IEEE, 2013.

[8] A. Al Hourani, S. Kandeepan, and A. Jamalipour, "Modeling Air-to-Ground Path Loss for Low Altitude Platforms in Urban Environments," in *IEEE, Global Communications Conference (GLOBECOM)*, pp. 2898–2904, Dec. 2014.

[9] J. Holis and P. Pechac, "Elevation Dependent Shadowing Model for Mobile Communications via High Altitude Platforms in Built-Up Areas," *IEEE Transactions on Antennas and Propagation*, vol. 56, no. 4, pp. 1078–1084, 2008.

[10] A. Al Hourani, S. Kandeepan, and S. Lardner, "Optimal LAP Altitude for Maximum Coverage," *IEEE, Wireless Communications Letters*, vol. 3, pp. 569–572, Dec. 2014.

[11] S. Chandrasekharan, S. Kandeepan, R. J. Evans, A. Munari, R. Hermenier, M.-A. Marchitti, and K. Gomez, "Clustering Approach For Aerial Base-Station Access With Terrestrial cooperation," in *Globecom Workshops (GC Wkshps), 2013 IEEE*, pp. 1397–1402, IEEE, 2013.

[12] M. Helmy, T. Baykaş, and H. Arslan, "Optimization of Aerial Base Station Location in LAP for Disaster Situations," in *IEEE Conference on Standards for Communications and Networking (CSCN)*, pp. 240–244, Oct. 2015.

[13] M. Helmy and H. Arslan, "Utilization of Aerial Heterogeneous Cellular Networks: Signal-To-Interference Ratio Analysis," in *JCN Special Issue on Amateur Drone and UAV Communications and Networks*, pp. 1–12, Under Review 2018.

[14] Cheng-Xiang Wang, F. Haider, Xiqi Gao, Xiao-Hu You, Yang Yang, Dongfeng Yuan, H. Aggoune, H. Haas, S. Fletcher, and E. Hepsaydir, "Cellular Architecture and Key Technologies for 5G Wireless Communication Networks," *IEEE, Communications Magazine*, vol. 52, pp. 122–130, February 2014.

[15] H. S. Jo, Y. J. Sang, P. Xia, and J. G. Andrews, "Heterogeneous Cellular Networks with Flexible Cell Association: A Comprehensive Downlink SINR Analysis," *IEEE Transactions on Wireless Communications*, vol. 11, pp. 3484–3495, October 2012.

[16] D. Liu, L. Wang, Y. Chen, M. Elkashlan, K.-K. Wong, R. Schober, and L. Hanzo, "User Association in 5G Networks: A Survey and an Outlook," *IEEE, Communications Surveys Tutorials*, vol. PP, no. 99, pp. 1–1, 2016.

[17] M. Helmy, Z. E. Ankaralı, M. Siala, T. Baykaş, and H. Arslan, "Dynamic Utilization Of Low-Altitude Platforms In Aerial Heterogeneous Cellular Networks," in *2017 IEEE 18th Wireless and Microwave Technology Conference (WAMICON)*, pp. 1–6, April 2017.

[18] B. T. Ahmed and M. C. Ramon, "Wimax In High Altitude Platforms (HAPs) Communications Over Large Cities," in *Systems, Signals and Devices, 2009. SSD'09. 6th International Multi-Conference on*, pp. 1–4, IEEE, 2009.

[19] I. Telecommunication Union (ITU), "Itu overview." `http://www.itu.int/en/ITU-T/publications/Pages/default.aspx`, 2012.

[20] D. Avagnina, F. Dovis, A. Ghiglione, and P. Mulassano, "Wireless Networks Based On High-Altitude Platforms For The Provision Of Integrated Navigation/Communication Services," *IEEE Communications Magazine*, vol. 40, no. 2, pp. 119–125, 2002.

[21] F. Dovis and F. Sellone, "Smart Antenna System Design For Airborne GSM Base-Stations," in *Sensor Array and Multichannel Signal Processing Workshop. 2000. Proceedings of the 2000 IEEE*, pp. 429–433, IEEE, 2000.

[22] F. De Rango, M. Tropea, A. F. Santamaria, and S. Marano, "Multicast QoS Core-Based Tree Routing Protocol And Genetic Algorithm Over An HAP-Satellite Architecture," *IEEE Transactions on Vehicular Technology*, vol. 58, no. 8, pp. 4447–4461, 2009.

[23] I. Bucaille, S. Hethuin, T. Rasheed, A. Munari, R. Hermenier, and S. Allsopp, "Rapidly Deployable Network For Tactical Applications: Aerial Base Station With Opportunistic Links For Unattended And Temporary Events Absolute Example," in *Military Communications Conference, MILCOM 2013-2013 IEEE*, pp. 1116–1120, IEEE, 2013.

[24] F. Dovis, R. Fantini, M. Mondin, and P. Savi, "4G Communications Based On High Altitude Stratospheric Platforms: Channel Modeling And Performance Evaluation," in *Global Telecommunications Conference, 2001. GLOBECOM'01. IEEE*, vol. 1, pp. 557–561, IEEE, 2001.

[25] T. W. East, "A Self-Steering Array For The SHARP Microwave-Powered Aircraft," *IEEE Transactions on Antennas and Propagation*, vol. 40, no. 12, pp. 1565–1567, 1992.

[26] M. Mondin, F. Dovis, and P. Mulassano, "On The Use Of HALE Platforms As GSM Base Stations," *IEEE Personal Communications*, vol. 8, no. 2, pp. 37–44, 2001.

[27] FACEBOOK, "Facebook takes flight." `https://www.theverge.com/a/mark-zuckerberg-future-of-facebook/aquila-drone-internet`, 2014.

[28] Google, "Broadband internet access to the developing world." `http://ravenaerostar.com/about/project-loon-raven-aerostargoogle`, 2014.

[29] G. Baldini, S. Karanasios, D. Allen, and F. Vergari, "Survey Of Wireless Communication Technologies For Public Safety," *IEEE Communications Surveys & Tutorials*, vol. 16, no. 2, pp. 619–641, 2014.

[30] S. Kandeepan, K. Gomez, L. Reynaud, and T. Rasheed, "Aerial-Terrestrial Communications: Terrestrial Cooperation And Energy-Efficient Transmissions To Aerial Base Stations," *IEEE Transactions on Aerospace and Electronic Systems*, vol. 50, no. 4, pp. 2715–2735, 2014.

[31] Y. Wei, L.-H. Li, W.-L. Sun, and W. Ying, "Energy-Efficient Relay Selection And Optimal Relay Location In Cooperative Cellular Networks With Asymmetric Traffic," *The Journal of China Universities of Posts and Telecommunications*, vol. 17, no. 6, pp. 80–88, 2010.

[32] D.-T. Ho, E. I. Grotli, P. Sujit, T. A. Johansen, and J. B. De Sousa, "Performance Evaluation Of Cooperative Relay And Particle Swarm Optimization Path Planning For UAV And Wireless Sensor Network," in *Globecom Workshops (GC Wkshps), 2013 IEEE*, pp. 1403–1408, IEEE, 2013.

[33] A. Aziz, I. Joe, and Y. Choi, "A Localization Algorithm For Disaster Situation Using Flying Sensor Nodes," in *Information Science and Applications (ICISA), 2014 International Conference on*, pp. 1–4, IEEE, 2014.

[34] L.-p. Zhu, Z. Chen, and Y.-S. Zhu, "Shadowing Fade Margin And Coverage Probability Analysis For HAP Mobile Communication Systems," *International Journal of Communication Systems*, vol. 27, no. 3, pp. 422–429, 2014.

[35] B. Błaszczyszyn, M. Jovanovicy, and M. K. Karray, "How User Throughput Depends On The Traffic Demand In Large Cellular Networks," in *Modeling and Optimization in Mobile, Ad Hoc, and Wireless Networks (WiOpt), 2014 12th International Symposium on*, pp. 611–619, IEEE, 2014.

[36] S. S. Szyszkowicz, H. Yanikomeroglu, and J. S. Thompson, "On The Feasibility Of Wireless Shadowing Correlation Models," *IEEE Transactions on Vehicular Technology*, vol. 59, no. 9, pp. 4222–4236, 2010.

[37] J. D. Parsons, *The Mobile Radio Propagation Channel*. Wiley, 2000.

[38] M. Mozaffari, W. Saad, M. Bennis, and M. Debbah, "Efficient Deployment Of Multiple Unmanned Aerial Vehicles for Optimal Wireless Coverage," *arXiv preprint arXiv:1606.01962*, 2016.

[39] V. V. C. Ravi and H. S. Dhillon, "Downlink Coverage Probability In A Finite Network Of Unmanned aerial vehicle (uav) base stations," in *IEEE 17th International Workshop on Signal Processing Advances in Wireless Communications (SPAWC)*, pp. 1–5, 2016.

[40] S. S. Szyszkowicz, F. Alaca, H. Yanikomeroglu, and J. S. Thompson, "Efficient Simulation Using Shadowing Fields Of Many Wireless Interferers With Correlated Shadowing," in *IEEE 71st, Vehicular Technology Conference (VTC)*, pp. 1–5, 2010.

[41] M. Vazquez-Castro, F. Perez-Fontan, and S. Saunders, "Shadowing Correlation Assessment And Modeling For Satellite Diversity In Urban Environments," *International Journal of Satellite Communications*, vol. 20, no. 2, pp. 151–166, 2002.

[42] Z. Han, A. L. Swindlehurst, and K. R. Liu, "Optimization of MANET Connectivity Via Smart Deployment/Movement of Unmanned Air Vehicles," *IEEE Transactions on Vehicular Technology*, vol. 58, no. 7, pp. 3533–3546, 2009.

[43] S. A. W. Shah, T. Khattab, M. Z. Shakir, and M. O. Hasna, "Association of Networked Flying Platforms With Small Cells For Network Centric 5G+ C-RAN," *arXiv preprint arXiv:1707.03510*, 2017.

[44] E. Kalantari, I. Bor-Yaliniz, A. Yongacoglu, and H. Yanikomeroglu, "User Association and Bandwidth Allocation For Terrestrial and Aerial Base Stations With Backhaul Considerations," *arXiv preprint arXiv:1709.07356*, 2017.

[45] B. Galkin, J. Kibiłda, and L. A. DaSilva, "A Stochastic Geometry Model of Backhaul and User Coverage in Urban UAV Networks," *arXiv preprint arXiv:1710.03701*, 2017.

[46] J. G. Andrews, F. Baccelli, and R. K. Ganti, "A Tractable Approach to Coverage and Rate in Cellular Networks," *IEEE Transactions in Communications*, vol. 59, no. 11, pp. 3122–3134, 2011.

Appendix A

Dynamic Utilization of LAPs in Aerial Heterogeneous Cellular Networks

A.1 Proof of Lemma 1

Let z be the index of the platform in which the user is associated with. Hence, the probability of the u user to be associated with the ABS in the i^{th} platform, i.e $z = i$, is given as

$$P_u(i) = \mathbb{P}[z = i] = \mathbb{E}_{D_{u,i}}[\mathbb{P}[\gamma_{u,i} > \max_{j,j\neq i} \gamma_{u,j}], \tag{A.1}$$

where $\mathbb{E}_{D_{u,i}}$ is averaging over $D_{u,i}$. From (1), $P_u(i)$ can be written as

$$\begin{aligned} P_u(i) &= \mathbb{E}_{D_{u,i}}[\prod_{\substack{j=1 \\ j\neq i}}^{K} \mathbb{P}[P_i D_{u,i}^{-\alpha_i} > P_j D_{u,j}^{-\alpha_j}]] \\ &= \mathbb{E}_{D_{ui}}[\prod_{\substack{j=1 \\ j\neq i}}^{K} \mathbb{P}[D_{uj} > (\frac{P_j}{P_i})^{\frac{1}{\alpha_j}} D_{ui}^{\frac{\alpha_i}{\alpha_j}}]] \\ &= \int_0^{\infty} \left[\prod_{\substack{j=1 \\ j\neq i}}^{K} \mathbb{P}[D_{uj} > (\frac{P_j}{P_i})^{\frac{1}{\alpha_j}} D_{ui}^{\frac{\alpha_i}{\alpha_j}}] \mathbf{f}_{D_{ui}}(d) dd, \right. \end{aligned} \tag{A.2}$$

where $\mathbf{f}_{D_{ui}}(d)$ is the PDF of D_{ui}. This PDF of D_{ui} can be derived by the null probability of the 2-D Poisson process [46]. We have

$$\begin{aligned}&\mathbb{P}[D_{ui} > d] \\ &= \begin{cases} \mathbb{P}[R_{ui} > \sqrt{d^2 - h_i^2}] = e^{-\lambda_i \pi (d^2 - h_i^2)}, & \text{for } d \geq h_i \\ 0, & \text{for } 0 \leq d < h_i \end{cases}\end{aligned} \tag{A.3}$$

leading to the PDF which can be found as

$$\mathbf{f}_{D_{ui}}(d) = \begin{cases} 2\,\pi\,\lambda_i\,d\,e^{-\lambda_i \pi (d^2 - h_i^2)}, & \text{for } d \geq h_i \\ 0, & \text{for } 0 \leq d < h_i \end{cases} \tag{A.4}$$

Hence, we can write

$$\begin{aligned}&\prod_{\substack{j=1 \\ j \neq i}}^{K} \mathbb{P}[D_{uj} > \left(\frac{P_j}{P_i}\right)^{\frac{1}{\alpha_j}} d_i^{\frac{\alpha_j}{\alpha_i}}] = \\ &\begin{cases} \prod\limits_{\substack{j=1 \\ j \neq i}}^{K} e^{-\lambda_j \pi (\tilde{P}_j)^{\frac{2}{\alpha_j}} (d^2 - h_i^2)^{\frac{1}{\alpha_j}}}; & \text{for } \prod\limits_{\substack{j=1 \\ j \neq i}}^{K} \left(\tilde{P}_j\right)^{\frac{1}{\alpha_j}} d^{\frac{1}{\alpha_j}} \geq h_i \\ 0; & \text{for } 0 \leq \prod\limits_{\substack{j=1 \\ j \neq i}}^{K} \left(\tilde{P}_j\right)^{\frac{1}{\alpha_j}} d^{\frac{1}{\alpha_j}} < h_i \end{cases}\end{aligned} \tag{A.5}$$

By substituting (40) and (41) into (38) we get

$$\begin{aligned}P_u(i) = \int_{h_i}^{\infty} \Big[&2\pi\lambda_i d \exp\{-\pi \sum_{\substack{j=1 \\ j \neq i}}^{K} \lambda_j (\tilde{P}_j)^{\frac{2}{\alpha_j}} (d^2 - h_i^2)^{\frac{1}{\alpha_j}} \\ &- \pi\lambda_i (d^2 - h_i^2)\}\Big] dd,\end{aligned} \tag{A.6}$$

For $j = i$, we can get $\sum\limits_{j=1, j \neq i}^{K} \lambda_j (\tilde{P}_j)^{\frac{2}{\alpha_j}} (d^2 - h_i^2)^{\frac{1}{\alpha_j}} - \lambda_i (d^2 - h_i^2) = \sum\limits_{j=1}^{K} \lambda_j (\tilde{P}_j)^{\frac{2}{\alpha_j}} (d^2 - h_i^2)^{\frac{1}{\alpha_j}}$. From (42), we obtain the result in (2).

Since the HAP and the LAP platforms experience the same environment, we can assume a common path loss exponent for both of them, i.e. $\alpha_j = \alpha \;\forall\; j \in \{1, ..., K\}$. Hence, by

integrating, we can express the user association probability as

$$P_u(i) = \frac{\lambda_i}{\sum\limits_{j=1, j\neq i}^{K} \lambda_j (\tilde{P}_j)^{\frac{2}{\alpha}} + \lambda_i}. \tag{A.7}$$

A.2 Proof of Theorem 2

The outage probability of the i^{th} platform is is given by

$$\begin{aligned} P_{OUT}(i) &= 1 - \int_0^{\infty} \mathbb{P}[SIR_i(x) > T] \mathbf{f}_{X_i}(x) dx \\ &= 1 - \frac{2\pi\lambda_i}{P_u(i)} \int_0^{\infty} \mathbb{P}[SIR_i(x) > T] \\ &\quad \Big[x \exp\{-\pi \sum_{j=1}^{K} \lambda_j (\tilde{P}_j)^{\frac{2}{\alpha_j}} (x^2 - h_i^2)^{\frac{1}{\alpha_j}} \} \Big]. \end{aligned} \tag{A.8}$$

The CCDF of the *SIR* at distance x from the typical user to its associated ABS in i^{th} platform is given as

$$\mathbb{P}[SIR_i(x) > T] = \mathbb{P}[q_{i,u} > P_i^{-1} |x|^{\alpha_i} T \sum_{\substack{j=1 \\ j\neq i}}^{K} P_j q_{j,u} |D_{u,j}|^{-\alpha_j}], \tag{A.9}$$

Let $Y = \sum\limits_{\substack{j=1 \\ j\neq i}}^{K} I_j$ be a total interference from all interfering ABSs, since $I_j = P_j q_{j,u} |D_{u,j}|^{-\alpha_j}$.
Hence, we can rewrite the CCDF of the SIR as

$$\begin{aligned} \mathbb{P}[SIR_i(x) > T] &= \mathbb{P}[q_{i,u} > P_i^{-1} |x|^{\alpha_i} T\ Y] \\ &= \int_0^{\infty} \exp\{-P_i^{-1} |x|^{\alpha_i} T\ y\} \mathbf{f}_Y(y) dy \\ &= \mathbb{E}_Y[\exp\{-P_i^{-1} |x|^{\alpha_i} T\ y\}] \\ &= \prod_{j=1, j\neq i}^{K} \mathscr{L}_{I_j}(P_i^{-1} |x|^{\alpha_i} T), \end{aligned} \tag{A.10}$$

where $\mathscr{L}_{I_j}$ is the Laplace transform of I_j and given as

$$\begin{aligned}
&\mathscr{L}_{I_j}(P_i^{-1}|x|^{\alpha_i}T) = \\
&\quad \mathbb{E}_{\phi_j}[\prod_{w\in\phi\setminus\{0\}} \exp\{\frac{P_j}{P_i}x^{\alpha_i}T\ q_{j,w}|D_{j,w}|^{-\alpha_j}\}] \\
&= \exp\{2\pi\lambda_j \int_{k_j}^{\infty}(1-\mathscr{L}_{q_j}(|x|^{\alpha_i}\tilde{P}_j T\ d^{-\alpha_j}))d\ dd\} \\
&\quad = \exp\{2\pi\lambda_j \int_{k_j}^{\infty} \frac{d}{1+(x^{\alpha_i}\tilde{P}_j T\ )^{-1}d^{-\alpha_j}}dd\},
\end{aligned} \tag{A.11}$$

where $k_j = (\tilde{P}_j)^{\frac{1}{\alpha_j}}x^{\tilde{\alpha}_j}$ is the closest interference from the j^{th} platform. By making a change of variables $v = (x^{\alpha_i}\tilde{P}_j T)^{\frac{2}{\alpha_j}}d^2$, the integral can be expressed as

$$\int_{k_j}^{\infty} \frac{d}{1+(x^{\alpha_i}\tilde{P}_j T\ )^{-1}(d)^{\frac{-\alpha_j}{2}}}dr = \int_{T^{\frac{-2}{\alpha_j}}}^{\infty} \frac{dv}{1+v^{\frac{\alpha_j}{2}}}, \tag{A.12}$$

Thus, we can express the Laplace transform of I_j as

$$\mathscr{L}_{I_j}(P_i^{-1}|x|^{\alpha_i}T) = \exp\{2\pi\lambda_j \mathbb{A}(\alpha_j, T)\}, \tag{A.13}$$

where,

$$\mathbb{A}(\alpha_j, T) = \frac{2\ T^{\frac{-2}{\alpha_j}+1}}{\alpha_j - 2}\,{}_2\mathrm{F}_1[1, 1-\frac{2}{\alpha_j}; 2-\frac{2}{\alpha_j}; -T], \tag{A.14}$$

where ${}_2\mathrm{F}_1[a,b;c;z]$ denotes the Gauss hyper-geometric function. Combining (49) into (46), gives

$$\mathbb{P}[SIR_i(x) > T] = \exp\{-\pi \sum_{\substack{j=1 \\ j\neq i}}^{K} \lambda_j \mathbb{A}(\alpha_j, T)\}, \tag{A.15}$$

After combining (51) and (41), we get the outage probability for i^{th} platform in (20).

Appendix B

Acronyms

3G Third Generation

4G Fourth Generation

5G Fifth Generation

ABS Air Base Station

ATG air-to-ground

ABSOLUTE Aerial Base Stations with Opportunistic Links For Unexpected and Temporary Events

AWGN Additive White Gaussian Noise

AHCN Aerial Heterogeneous Cellular Networks

HCN Heterogeneous Cellular Networks

BER Bit Error Rate

FBWA Fixed broadband wireless access

BRS Broadband Radio Service

BS Base Station

CDF	Cumulative Distribution Function
PDF	probability density function
LOS	Line Of Sight
NLOS	Non Line Of Sight
HAP	High Altitude Platforms
LAP	Low Altitude Platforms
UAV	Unmanned Aerial Vehicle
Wi-Fi	Wireless Fidelity
WiMAX	Worldwide Interoperability for Microwave Access
LTE-A	Long Term Evolution-Advanced
LTE	Long Term Evolution
GSM	Global System for Mobile communications
WRC	World Radiocommunication Conference
LEO	Low Earth Orbit
ITU	International Telecommunication Union
ITU-R	International Telecommunications Union-Radiocommunication Sector
HALE	High Altitude Long Endurance-Demonstrator
QoS	Quality of Service
SNR	Signal to Noise Ratio
SIR	Signal to Interference Ratio
UHF	Ultra High Frequency
RSS	Received Signal Strength

DL	Downlink
FSPL	Free Space Path Loss
HDTV	High-Denition Television
MMDS	Multi-Channel Multimedia Distribution Service
GPRS	General Packet Radio service system
UMTS	Universal Mobile Telecommunications System
WCDMA	Wideband Code Division Multiple Access
IMT	International Mobile Telecommunications
SHARP	Stationary High Altitude Relay Platform
SHF	super high frequency
HALEP	High-Altitude Long Endurance Platform
PPDR	Public Protection and Disaster Relief
PL	pathloss
RATs	radio access technologies
FSO	Free Space Optical
PPP	point Poisson process

AERIAL PLATFORMS UTILIZATION FOR FUTURE NETWORKS

ORIGINALITY REPORT

15%	11%	11%	2%
SIMILARITY INDEX	INTERNET SOURCES	PUBLICATIONS	STUDENT PAPERS

PRIMARY SOURCES

1	researchbank.rmit.edu.au Internet Source	2%
2	Jo, Han-Shin, Young Jin Sang, Ping Xia, and Jeffrey G. Andrews. "Heterogeneous Cellular Networks with Flexible Cell Association: A Comprehensive Downlink SINR Analysis", IEEE Transactions on Wireless Communications, 2012. Publication	1%
3	arxiv.org Internet Source	1%
4	Submitted to Higher Education Commission Pakistan Student Paper	<1%
5	qmro.qmul.ac.uk Internet Source	<1%
6	www.cordis.europa.eu Internet Source	<1%